Reconsidering the glaciogenic origin of Gondwana diamictites of the Dwyka Group, South Africa

Mats O. Molén[1]*, J. Johan Smit[2]

[1] UmeåFoU AB, Vallmov 61, 903 52 Umeå, Sweden
[2] 9 Gradwell Street, Parys 9585, South Africa
* corresponding author, e-mail: mats.extra@gmail.com

Abstract

The Gondwana Late Palaeozoic Ice Age is probably best represented by the Dwyka Group in South Africa. Striated and grooved surfaces or pavements are commonly considered to have formed subglacially, as are diamictites which have been interpreted as *in-situ* or reworked tillites. These interpretations were tested by investigation of outcrops in formerly well-studied areas, throughout South Africa. Detailed analyses have focused on striated surfaces/pavements and surface microtextures on quartz sand grains in diamictites. The sedimentological context of four pavements, interpreted to be glaciogenic, display features commonly associated with sediment gravity flows, rather than glaciation. A total of 4,271 quartz sand grains were subsampled from outcrops that are considered mainly to be tillites formed by continental glaciation. These grains, analysed by SEM, do not demonstrate the characteristic surface microtexture combinations of fracturing and irregular abrasion associated with Quaternary glacial deposits, but mainly a mix of surface microtextures associated with multicyclical grains. The Dwyka Group diamictites warrant reinterpretation as non-glacial sediment gravity flow deposits.

Key words: Surface microtexture, sediment gravity flow, Late Palaeozoic Ice Age, pavement, Nooitgedacht

1. Introduction

1.1. Process-related geology

The research question in the present study is whether the geological features in the Dwyka Group of South Africa indicate glacial conditions or not.

Schermerhorn (1974, 1976a, 1976b, 1977) published a comprehensive review which documented evidence for a sediment gravity flow origin of ancient tillites, shown in his classic work on Late Precambrian diamictites, even though an older paper by Crowell (1957) is considered to be the first to have covered this research area. Since then there has been a growing understanding that many pre-Pleistocene glaciogenic deposits could have been formed by different kinds of slumps, slides and sediment gravity flows like turbidity currents, and especially by cohesive debris flows (e.g., Eyles, 1993; Eyles & Januszczak, 2007; Vesely et al., 2018; Fedorchuk et al., 2019; Kennedy & Eyles, 2021).

In this context the origin of the Permo-Carboniferous Dwyka Group diamictites of South Africa was studied. As most documentation of the general geology of the Dwyka Group formerly published does not need discussion, only geological features which are particularly important for the origin of the deposits were examined in detail. Independent of the process – glaciation or sediment gravity flow – the source and age of the sediments will be similar, e.g., data published by Griffis et al. (2021) and interpreted in a glaciogenic context still hold, even if the process may be different.

Commonly, researchers start with the interpretation that the Dwyka Group is to a large part glaciogenic, as this is the current understanding of the geological features. In the present work the starting assumption is the evidence from geological processes of Pleistocene and recent glaciations, i.e., a process-related issue (Shanmugam, 2021; Molén, 2022a, 2022b), and not former interpretations. The most distinctive geological feature from the Dwyka Group interpreted to be glaciogenic is striated and grooved surfaces, i.e., 'glacial pavements'. Therefore, a sample of well-known striated surfaces was studied in detail and compared to striated surfaces produced by Quaternary glaciers and by sediment gravity flows (e.g., Peakall et al., 2020). Furthermore, surface microtextures on quartz grains will display evidence of any glaciogenic transport history of diamictites, even if sediments had been reworked by, for instance, slides or sediment gravity flows (Mahaney, 2002; Molén, 2014). Therefore, to uncover the transport history of the Dwyka Group diamictites, quartz sand grains were studied by SEM.

1.2. Origin of geological features – glaciogenic or related to sediment gravity flows

Differences between glaciogenic and mass flow features often can be revealed by comparing data from different geological disciplines (compare Shanmugam et al., 1994; Major et al., 2005; Talling et al., 2007, 2012; Dakin et al., 2013; Shanmugam, 2016; Molén, 2017, 2021, 2022a, 2022b; Dietrich & Hofmann, 2019; Peakall et al., 2020; Cardona et al., 2020). Geological features which are commonly interpreted as glaciogenic, for example, striated, grooved and polished bedrock, including all kinds of chevron structures/crescentic gouges/chattermarks, grooves and nailhead striations, can form as a result of different kinds of mass movements, such as avalanches, slides and different kinds of sediment gravity flows (Draganits et al., 2008; Dakin et al., 2013; Molén, 2017, 2021, 2022a, 2022b; Kennedy & Eyles, 2021). A lahar generated by the Mount St. Helens eruption truncated volcanic boulders and produced, in places "... a surface similar to a glacial pavement cut in conglomerate" (Scott, 1988, p. A43). A process somewhat similar to glacial plucking may be caused by sediment gravity flows, and sometimes by fluvial action, even on the face of hard granite (Whipple et al., 2000; Dakin et al., 2013; Kennedy & Eyles, 2021; Molén, 2022a).

1.3. Geology of the Dwyka Group

1.3.1. History of research, tectonic context and evidence of sediment gravity flows

The Dwyka Group is present mainly in large basins, the Karoo Basin of South Africa and the Aranos/Kalahari Basin, the main part in Botswana and Namibia. The unit is conformably overlain by the Ecca Group shales to a great depth (e.g., Baiyegunhi & Gwavava, 2016; Götz et al., 2018; Bell et al., 2020).

The Dwyka Group has to a large part been studied with the commonly accepted interpretation, or paradigm, that this sedimentary unit was the geological consequence of a major glaciation. In 1856 the diamictites were interpreted to be of volcanic origin (Sandberg, 1928; Norman, 2013), and later as mudflows or the result of meteorite impacts, including striated surfaces (Geophysical Discussion, 1960; Master, 2012; Rampino, 2017). The glaciogenic interpretation was first published in 1870 (Hancox & Götz, 2014), generally accepted in 1898 (Sandberg, 1928), and basically has withstood critical comments and alternative geological interpretations. During the early investigations of the Dwyka Group, most sections were considered to have been deposited subglacially, but as more data accumulated, interpretations have become more complicated, including many and varied glacial advances and retreats, and recognising the presence of sediment gravity flows and rain-out deposits (Visser, 1986, 1990, 1994, 1996, 1997; Visser et al., 1997a, 1997b; Isbell et al., 2008; Dunlevey & Smith, 2011).

The current work is mainly concerned with the Karoo Basin, an area which was primarily controlled by tectonism (Von Brunn, 1994; Visser, 1997; Bangert & Von Brunn, 2001; Isbell et al., 2008). Partly overlapping, and extending outside of the time period of the deposition of the Dwyka Group, large compressional events are associated with the Cape orogeny (Scheiber-Enslin et al., 2015). In the southern part of South Africa, the Dwyka Group was tectonically deformed during uplift and partially metamorphosed (Fagereng, 2014). In conclusion, the Karoo Basin shows evidence of downwarping as a lithospheric deflection (Dietrich & Hofmann, 2019). The basin may be seen as a retroarc foreland basin, and the Dwyka Group forms its basal part (Johnson et al., 1997; Catuneanu et al., 2005; Barbolini et al., 2018; Hansen et al., 2019; Dietrich & Hofmann, 2019).

In areas with Dwyka Group sediments in Namibia, interpreted to be subglacial, the basal unconformity below diamictites may be highly irregular and heterogenous, with areas of sediment injections into the underlying basement, and 'elongated boul-

ders' of sediment displaying fractures (Le Heron et al., 2021), i.e., an appearance partly similar to jigsaw-puzzle textures which are common in sediment gravity flow deposits (Dufresne et al., 2021; Molén 2021). Furthermore, in Namibia, Martin (1981) described 'pre-glacial valleys' that were glaciated and also crossed obliquely by glaciers. As the valleys are interpreted to be mainly pre-glacial, perhaps originating by tectonism and glaciated during the Neoproterozoic (Bechstädt et al., 2018), it may be difficult to determine if there is any impact from more recent glaciers, as the pre-glacial appearance is still present. The descriptions of these valleys are general glaciogenic interpretations of different geological features (Dietrich et al., 2021), but details which have not been documented may often reveal alternative interpretations of, for example, striations and roches moutonnées (Molén, 2022a, 2022b). Namibian ('pre-glacial') valleys do not display typical characteristics of fjords (i.e., no ridge at the outlet and not narrow), despite the fact that it may be the current interpretation (Dietrich et al., 2021). Valleys in northern South Africa have uneven floors (Visser, 1987). The Virginia Valley (Orange Free State), which has been described as a fjord, does not display the typical narrowness, overdeepening and a prominent "sill" or ridge at the outlet, so typical of fjords (Mangerud et al., 2019), but is a rather wide and shallow valley (Visser & Kingsley, 1982). Hanging valleys, including in magmatic/metamorphic bedrock, are often present in subaqueous and other non-glacial canyons (Dill, 1964; Shepard & Dill, 1966; Mitchell, 2006; Amblas et al., 2011; Normandeau et al., 2015), and are not exclusive to glaciation. Hanging valleys that have been reported from the Dwyka Group may therefore be interpreted to be non-glacial (Visser, 1982; Hancox & Götz, 2014). U-shaped valleys commonly form by non-glacial processes, so the shape by itself is not evidence of glaciation (Amblas et al., 2011; Puga Bernabéu et al., 2020).

The Dwyka Group sediments consist of very complex layered successions with many diamictites, sandstones and shales superimposed or interfingering with and/or eroded into each other (Visser et al., 1987; Visser & Loock 1982, 1988; Visser, 1988, 1989a, 1989b; Dietrich & Hofmann, 2019), similar to and often interpreted to be sediment gravity flow deposits. The glaciogenic outcrops both in South Africa and South America, have lately been reinterpreted to have originated from many smaller glaciers and not one large glacier that was continuous and covered large parts of Gondwana (Dietrich et al., 2019; Fedorchuk et al., 2019), even though there is still an ongoing discussion (Craddock et al., 2019;

Griffis et al., 2021). Therefore, reinterpretation of the Dwyka Group diamictites may not affect the interpretation of any other Gondwana diamictites, as the glaciation at any rate is considered to be patchy or discontinuous during its long duration. Massive diamictites have been discovered to be often stratified and to be aprons, fans or debris flows and not deposited subglacially (Visser, 1994, 1997; Visser et al., 1997a; Huber et al., 2001; Haldorsen et al., 2001; Isbell et al., 2008; Dietrich & Hofmann, 2019; Johan Visser, pers. comm., 2020), and some authors believe that there are only very few places where there is subglacial basal/lodgement tillite (Visser, 1997; Isbell et al., 2008), while others are more likely to interpret diamictites as subglacially formed (e.g., Blignault & Theron, 2015). Horan (2015) reinterpreted much of the Dwyka Group as having been deposited in a large lake. All these new interpretations and data make it difficult to know what is considered to be primarily glaciogenic.

Where massive diamictite rests on igneous (or metamorphic) bedrock, there are often large areas displaying a thin layer (maximum 1 m in thickness) superimposed on the bedrock of brecciated and reworked, but not (heavily) abraded bedrock material, similar to what may also be present discontinuously at the base of cohesive sediment gravity flows (Festa et al., 2016). In addition, there is evidence of soft sediment deformation or thinly bedded sedimentary deposits superposed on the breccia (Visser, 1981, 1997; Isbell et al., 2008), indicating a less powerful environment than underneath a glacier and similar to facies produced by sediment gravity flows. Such a sequence may be interpreted as tectonic shattering of the bedrock followed by sediment gravity flows (Molén, 2021). However, brecciation may also be formed in the basal shear zone below mass flows (Cardona et al., 2020), while bedrock in the subglacial environment is plucked and heavily abraded.

1.3.2. Dropstones and palaeotransport
Outsized clasts which are generally interpreted as dropstones are present in the Dwyka Group and are commonly small (Tavener-Smith & Mason, 1983). Solitary clasts, well rounded or angular, which are enclosed by sediments with a similar appearance as around dropstones, commonly are also transported by floating vegetation and in sediment gravity flows. There are boulders up to 70 kg in Carboniferous coal seams (Price, 1932; Liu & Gastaldo, 1992), and boulders transported by modern floating (commonly larger) tree roots are up to 3 m (Bennett et al., 1996). From Cretaceous and Carboniferous sedimentary rocks, boulders were described

that were transported over up to 100 km by floating vegetation (Hawkes, 1943; Liu & Gastaldo, 1992). But, more importantly, there is commonly an abundance of clasts, occasionally in sizes up to metres in diameter, within sediment gravity flow deposits and embedded in a clayey and in instances rhythmic matrix (e.g., Bouma, 1964; Embley, 1982; Molén, 2017, 2021, 2022a; Peakall et al., 2020). If the 'dropstones' only display evidence of sediment draping and compaction, it may indicate a sediment gravity flow. If there is penetration of clasts, these may have been dropped by an agent but may also have been transported by sediment gravity flows (Kennedy & Eyles, 2021; Molén, 2021, 2022a, 2022b). Tavener-Smith & Mason (1983) and Haldorsen et al. (2001) documented 'dropstones' from South Africa which are mainly draped by or within single strata of rhythmites or other sedimentary strata, and Visser (1983b) described outsized clasts in debris flow deposits, none that is different from occurrences of outsized clasts in non-glaciogenic deposits (e.g., Molén, 2017, 2021; Kennedy & Eyles, 2021).

Rhythmites in the Dwyka Group have been interpreted to be deposited from turbidity currents or tidal activity (Isbell et al., 2008). Within the diamictites, in what is described as the northern valley facies association of the Dwyka Group, most clasts are local. In what is described as the southern platform facies association (downstream from the northern valley facies) there is more far-transported material (Visser & Loock, 1982; Visser, 1986).

Palaeoslopes in the area are commonly referred to, but seldom measured (e.g., Visser et al., 1997a), but there is no evidence of large areas with lower slopes than below that documented for sediment gravity flows or slides of 0.05–1°, in instances for up to distances of 1,000 km (Yincan et al., 2017; Shanmugam, 2021; Molén, 2022a).

1.3.3. Pavements/striated surfaces
Usually, striations and grooves on bedrock are curved and irregular below glaciers (Flint, 1961; Iverson, 1991). By contrast, they are often straight when caused by tectonism or slides, and they may be both straight and curved due to sediment gravity flows but commonly are parallel or sub-parallel (e.g., Lindsay, 1970; Schermerhorn, 1970, 1971; Savage, 1972; Deynoux & Trompette, 1976; Glicken, 1996; Peakall et al., 2020).

Soft-sediment striations and pavements are commonly produced below sediment gravity flows, including crossed striations up to 90°, and in rare cases below flow tills (which is a kind of sediment gravity flow) (Evenson et al., 1977; Kneller et al., 1991; Pickering et al., 1992; Dakin et al., 2013;

Molén, 2022a), covering areas of up to *c*. 300 km² and for distances in excess of 40 km (Peakall et al., 2020). Soft-sediment pavements have not been documented to form commonly (or not at all) by direct glacial action.

Striated surfaces are numerous within and underneath the Dwyka Group sediments, and are considered as probably the prime geological evidence of glaciation. Many of the Dwyka striated surfaces were formed in unconsolidated material (Dietrich & Hofmann, 2019; Le Heron et al., 2019), and striations and grooves are often parallel (e.g., Savage 1972). In soft sediments, striated surfaces which are interpreted to be glaciogenic are often superimposed, or stacked, in many layers above each other. Similar stacked surfaces with parallel striations are not known from Pleistocene deposits where it is known that glaciers were the final depositional agent. They are similar to so-called tectonic hydroplastic slickensides or internal grooves and striations that form in soft sand and mud (Enos, 1969; Petit & Laville, 1987; Simms, 2007; Cesta, 2015; Le Heron et al., 2014), but they are sometimes interpreted as internal movements in sand caused by overriding ice (Deynoux & Ghienne, 2004; Le Heron et al., 2005, 2019).

Commonly, the Dwyka Group striated surfaces/pavements display features which are strikingly different from Quaternary glacially striated surfaces. Six examples of such differences are:

a) Striations continue unbroken from on top of a 'tillite' into the striations on the pavement below (Flint, 1961).
b) Striations are present in triple superposed/stacked soft-sediment surfaces on top of a striated surface/pavement in Ventersdorp lava (Visser, 1988).
c) Thin soft sediment beds are present between striated pavement and diamictite (Slater et al., 1932; Visser, 1988; Visser & Loock, 1988).
d) A soft-sediment striated surface is cut into ripple laminated siltstone (Visser, 1983a).
e) Fossil plants are present on top of a striated pavement and compressed below 'tillite' (du Toit, 1926; Sandberg, 1928).
f) A soft-sediment striated surface is draped with mudrock with crustacean track ways, which passes up to diamictite (Von Brunn, 1996).

1.3.4. Interpreting climate data
Model calculations of pCO_2 during the Phanerozoic are inconclusive (Montañez et al., 2016; Myers, 2016; Dahl & Arens, 2020), and recent reviews of palaeotemperatures had to dismiss about half of the data to make it fit in with current interpretations of

palaeoclimate (Scotese et al., 2021). The $\delta^{13}C_{org}$ does not change in the post-glacial Ecca Formation which conformably overlies the Dwyka Group (Scheffler et al., 2003). The $\delta^{13}C_{org}$ in the Dwyka Group displays evidence of a primarily algal origin (Scheffler et al., 2003). Therefore, ^{13}C-discrimination cannot be used as a final answer for past CO_2 levels.

The fossil vegetation of the Late Carboniferous and Early Permian South Africa deposits does not include plants described as displaying physiological adaptations typical of cold or subpolar climate species (Anderson & McLachlan, 1976; McLoughlin, 2011; Hancox & Götz, 2014). Fossils of the *Glossopteris* flora are closely associated with the Dwyka Group diamictites, and have even been discovered between 'tillite' and the underlying 'ice-polished bedrock' (du Toit, 1926; Sandberg, 1928). Coalified plant fragments also occur within massive 'tillites', and coal seams are often situated superimposed on, or between, 'tillites' (Anderson & McLachlan, 1976; Stavrakis, 1986; Stavrakis & Smyth, 1991; Visser, 1989a; Hancox & Götz, 2014). Coal seams that may be interbedded with 'glaciogenic' diamictites have in many instances coalesced with other coal seams to form one thick coal seam (Stavrakis & Smyth, 1991). The mixing of diamictites and coal beds of the Dwyka Group may be considered to be a result of reworking (Hancox & Götz, 2014), but coal seams that are interbedded between stacked Dwyka diamictite deposits are often thin, and complete sequences appear to be a kind of debris flow deposits (Hancox & Götz, 2014). Some deposits may be considered to be hyperpycnite beds sorted into dense and diluted parts with or without plant material, and these deposits may later transform into a full spectrum of sediment gravity flows (Zavala & Arcuri, 2016; Shanmugam, 2019; Zavala, 2019, 2020). The absence of fossils in most parts of the Dwyka Group deposits may be an indication of water depth or transport distance, i.e., deeper water or sorting during longer transport. Fossils are seldom reported from within debris flow deposits, but in Holocene glaciogenic deposits there may be trees and other plants if these were growing nearby (Fleisher et al., 2006; Ryder & Thomson, 2011).
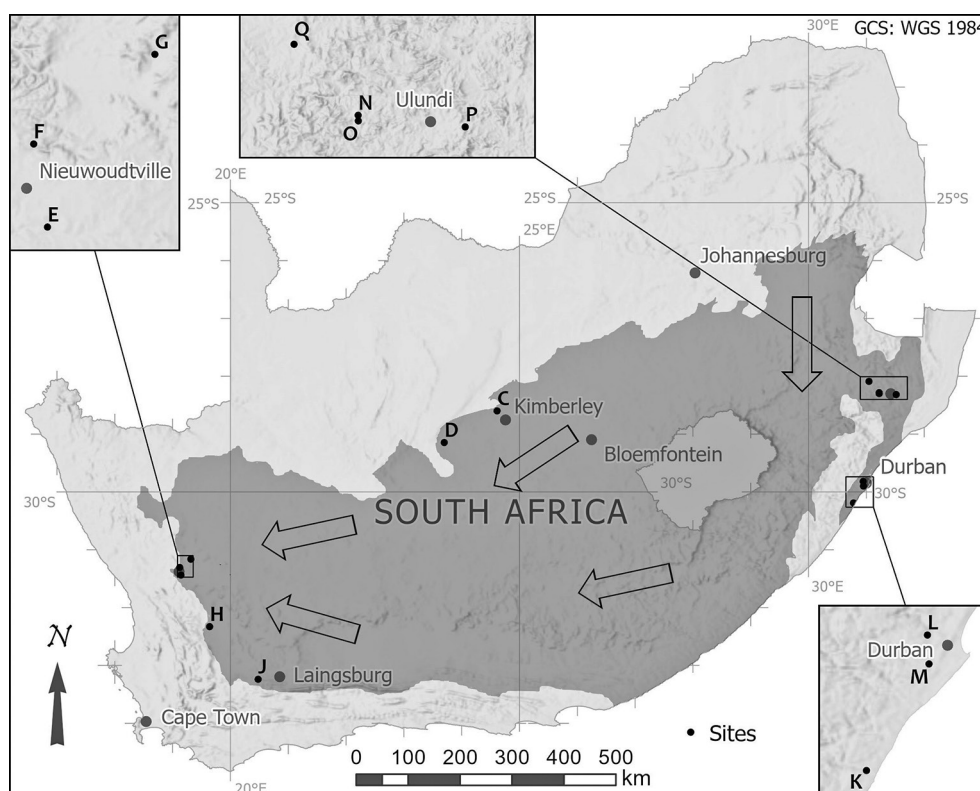

Fig. 1. Study area and field locations. C – Nooitgedacht, diamictite and striated surface, D – Douglas pavement, E – Oorlogskloof, soft-sediment pavement, F – Nieuwoudtville, G – Kransgat River, Koringhuis, H – Elandsvlei, J – Matjiesfontein, K – Umkomaas River Valley, L – Durban University of KwaZulu-Natal Westville Campus, M – Durban, Coedmore Quarry, N – west of Denny Dalton, O – south-west of Denny Dalton, P – east of Ulundi, Q – Surreyvale. The Karoo Basin is marked in a darker colour, approximately, after Catuneanu et al. (2005). General major ice-flow directions (arrows) are after Visser (1997), Cape Geosites (2014) and Dietrich & Hofmann (2019).

As most of the Dwyka Group has now been reinterpreted as 'glacial marine' deposits from a middle palaeolatitude far from the South Pole (Craddock et al., 2019; around 30–60°S as depicted by Kent & Muttoni, 2020), it has become difficult to distinguish these deposits from non-glacially derived sediment gravity flow deposits. Some parts of the widespread Permo-Carboniferous 'tillites' have previously been interpreted to have been deposited close to 30°S (John, 1979; Chumakov & Zharkov, 2002; Catuneanu et al., 2005; Kent & Muttoni, 2020), while at about the same time there were apparently no (or very limited in areal extent) glaciers at the Permo-Carboniferous South Pole in Antarctica (Isbell et al., 2012, 2013; Montañez & Poulsen, 2013; Craddock et al., 2019). Likewise, there was no glaciation in South Africa when it was at or close to the South Pole during the Devonian and Early Carboniferous, even though glaciation has been interpreted in South America at the same time (Ruban et al., 2007; Kent & Muttoni, 2020; Caputo & Santos, 2020). Thus, a polar position by itself does not indicate glaciation *per se*.

2. Research area

The general geology and stratigraphy of the Dwyka Group have been thoroughly documented by many researchers. The current work is based on these former descriptions of the research areas which will not be repeated here. The question is whether or not the current climatological interpretation is correct. Several documented diamictite and striated surface/pavement outcrops of the Dwyka Group were chosen for field work, in order to investigate features that might shed light on their origin. Samples for SEM research were collected from Dwyka diamictite deposits from geographically distant parts of South Africa, so as to cover both the northern and southern area. Whenever possible, samples were collected at different levels and outcrops. Striated surfaces were studied at Nooitgedacht, Douglas, Oorlogskloof and Durban.

All research areas are marked in Figure 1 and listed in Table 1 (detailed descriptions can be found in Supplemental material).

Table 1. General descriptions of all Dwyka Group samples. All samples consist of > 90% clay, silt and fine sand, except where noted otherwise. Details can be found in the Supplemental material.

C. Nooitgedacht, diamictite on Ventersdorp lava pavement	
C-1-1	Thin black hard diamictite crust on top of pavement
C1b, C2a C2b, C2bb, C2c, C3a, C3b, C3c, C4	Diamictite. C1b, C2b, C2c, C3b and C3c are stratified
C3bm	String 1–10 mm of sediment between pavement and diamictite
C4m	Black string 2–3 mm of sediment between pavement and diamictite
F. Nieuwoudtville	
F1a, F1aa, F1b, F2, F2b, F3a, F3b. F3c, F5	Diamictite. F5 is stratified
F4, F4b	Conglomerate
F4c	Weathered sandstone pebble in sample F4, i.e. source rock
G. Kransgat River, Koringhuis homestead/farm	
G1a, G1b, G1c, G2a, G2b, G2c	Diamictite
H. Elandsvlei farm area	
H1, H1a, H2b, H2c	Diamcitite
J. South of Matjiesfontein	
J1a, J1b, J1c, J1d	Diamcitite
K. Umkomaas River Valley	
K1a, K1b, K1bb, K1c, K2, K2b, K3b, K3c	Diamcitite
L. Durban, University of Kwazulu-Natal Westville Campus	
L1, L1b, L1br, L1c	Mainly sand and silt. Pavement
M. Durban, Coedmore Quarry	
M1, M2, M3, M4, M6	Extra hard, mainly clay. Black
N, O. Denny Dalton	
N1a, N2a, N2b, O1a, O2	Diamcitite
P. R66 at Ulundi	
P1, P1a, P3a, P3b, P5b, P5c, P5e, P5 norm., P5s	Diamictite. P5s is thin sandy string
Q. Surreyvale	
Q1, Q3	Diamcitite

3. Methods

Pavements were recorded and documented in the field, as reported in Results. SEM methods are described below.

3.1. SEM studies of surface microtextures on quartz sand grains

The generation of surface microtextures during glaciation is well documented (Mahaney, 2002; Molén, 2014, 2017). Even if the final deposition of sediments may be non-glaciogenic, e.g., sediment gravity flows or rainout till that do not reshape the complete grain surfaces and leave little or no imprint on the grain surfaces, the surface microtextures will display evidence of a former glaciogenic history (Molén, 2014). Only if grains were dumped onto the top of a glacier (supraglacial), or transported inside the ice (englacial) and never reached the basal part of the glacier, or in periglacial sediments, will typical glaciogenic surface microtextures not be generated (Molén, 2014, 2017; Woronko, 2016). Surface microtextures will originate quickly and in large numbers, only if it is an all penetrating and continuous energetic environment like below a glacier, and these surface microtextures will probably almost immediately display evidence of subglacial stress (Molén, 2014). In a less all-penetrating energetic environment there has to be an extended time period to create numerous surface microtextures. In sediment gravity flows the energy dissipation is momentous and more 'sporadic', which may create fractures on single grains but commonly not simultaneous irregular abrasion on the same fractured surfaces.

The methods used in the present study were especially detailed and designed to discover any evidence of mechanical and chemical artificial generation of surface microtextures during sampling and laboratory work, and also to remove any post-depositional grain coatings (see Supplemental material). The more general methods were documented in detail by Molén (2014), and SEM methods are briefly described in Tables 2 and 3.

In total 71 samples were processed for SEM (Table 1). Surface microtextures on quartz grains are best displayed on the size fraction 0.25–2 mm (Molén, 2014), and therefore this size fraction is analysed here. Commonly 30–50 grains were studied from each sample, and hundreds of grains from each research area, in order to detect and then avoid any possible anomalies in the subsamples. Detailed descriptions are documented in the Supplemental material.

3.1.1. Methodology for SEM studies and surface microtexture classification

The method used to study surface microtextures is based on geological processes and not only the general appearance of grain surfaces (Molén, 2014; Table 2). The surface microtextures are ordered in a 2-History Diagram, depending on the freshness of the grain surfaces (Table 3, Figs. 2–7), for interpretation and visual documentation of the geological history. This diagram, with enhancing connecting lines, also displays an easily distinguishable 'geological signature' of the appearance of each sample, which will not show up in a histogram or any other diagram (Molén, 2014). Definitions and labels are in accordance with Tables 2 and 3.

History-1 surface microtextures are defined as recent, i.e., they are defined as having been generated by the last geological process which shaped the grain surfaces, which except for weathering surface microtextures, appear to be fresh. History-2 includes all surfaces which display weathering that shaped the grain preceding the origin of the History-1 surface microtextures, and are labelled as F2, f2, A2, SP2, EN2 or C2.

The geological history of quartz grains starts with crystallisation from a magma or in a metamorphic rock (EN/C), then release from bedrock (F/f),

Table 2. The predominant processes that influence the surface of a quartz grain, and symbols/abbreviations for the different surface microtextures (details in Molén, 2014, but this table has in part been modified to include more variations of surface microtextures).

Mechanism	Microtexture	Environment
Crushing	large scale fractures (**F**)	glacial, tectonic, crystallisation, rock slide/fall, high energy environments
	small scale fractures (**f**)	water, glacial, wind, gravity flow
Abrasion	rounded edges, rounded microtextures, grooves (**A**)	water, glacial, wind, gravity flow
Chemical	solution, precipitation (**SP**)	weathering, contact reactions, lithification,
Crystal growth	embayments, nodes (**EN**)	metamorphism, crystallization
	crystal surfaces (**C**)	precipitation, lithification, crystallization

Table 3. Definition of surface microtextures (SM). Percentages are approximate and calculated from comparison of how large an area of the grain surface is covered by a surface microtexture. If, for example, many very small f1, about 4% or less coverage each, in total cover more than 10–15%, then both F1 and f1 are recorded as surface microtextures. There are many special small-scale fractures in this size, which are recorded in tills and other environments (Mahaney, 2002; Molén, 2014). The percentages of the History-2 surface microtextures are similar to the History-1 definitions, except that they are weathered.

SM	Area coverage	Excludes
F1	≥20–25%; or sum of many 5–20% **f1** covering ≥50–55%	**f1** (except if many ≤4% covering ≥10–15%); and **SP1** (except if sequence of origin is unknown)
f1	5–20%; or sum of many ≤4% covering ≥10–15%	
A1	≥15–20%	
SP1	≥10–15%	**SP2** (except if sequence of origin is evident)
EN1	≥10–15%	
C1	≥5–10%	
F2	see definition of **F1**	**f2**

transport (F/f/A) and weathering (SP), in different combinations. For example, weathered grains, released from bedrock and then abraded by ice will document large fresh fractures and (irregular) abrasion as the most recent geological history (History-1) and weathered surfaces and crystal surfaces from a previous history (History-2) of the host bedrock, i.e., F1, A1, SP2 and EN2 or C2. Small-scale fractures (f) often are of lesser genetic importance, as they easily originate from small forces/collisions and may almost always be hypothesised for History-2.

Some researchers may only record a few minute surface microtextures, which may originate in different environments, on a small sample of grains, as evidence to deduce an interpretation of the origin of a sedimentary deposit, while the overall appearance of all surface microtextures on a large number of grains in the deposit may indicate a different origin.

The quartz grains that were recorded in the current research were divided into two main groups, those with and without fresh F1-fractures, but only if F1 was the single surface microtexture in the most recent history and there were no other fresh surface microtextures such as EN1 or A1. The reason for this was twofold: first, it is unknown how many fractures are from a) depositional processes or from b) post-depositional processes like compression or recent anthropogenic road construction/mining work or sampling/laboratory processes, and, secondly, if there is a mix of grains displaying only F1-fractures as the most recent history together with grains displaying A1/SP1, this mixture of grains will skew the result in a 2-History Diagram (Molén, 2017). The A1/SP1 group was used in most analyses and interpretations of the geological history of the diamictites, as these had not acquired any single recent/final fracturing.

The SEM analysis of the Dwyka Group samples was conducted with a 'table top' Hitachi TM 3000 equipped with a backscattered electron detector for imaging and an energy dispersive X-ray spectrometer (Bruker, Quantax 70 system) for element analysis. Imaging was done at both 5 and 15 kV and element analysis at 15 kV with a high probe current.

4. Results

4.1. SEM studies of surface microtextures

4.1.1. Documentation of surface microtextures
The details of the laboratory processes and field data from all South African samples are documented in the Supplemental material.

The 71 Dwyka samples analysed included 4,271 quartz grains of size 0.25–2 mm. Of these 664 grains displayed F1 as the single most recent surface microtexture (and no other History-1 surface microtextures). In the present study 3,110 grains from diamictites which have been interpreted as tillites or reworked tillites, which had not been simply fractured (i.e., no single F1), displayed A1/SP1 for between 96–100% of the grains (Fig. 7). These grains also displayed f1 (9–24%) and/or only SP1 with no abrasion. Other sediments, i.e., those in between the striated surface and diamictite (samples C3bm and C4m), a small conglomerate (samples F4-F4c) and sandstone (samples L1-L1c), displayed 83–100% A1/SP1.

4.1.2. Comparison of surface microtextures of South African diamictites to Quaternary glacial deposits
In order to reveal any similarities to till, quartz grains from the South African diamictites were

compared to quartz grains deposited from Quaternary glaciers (Figs. 2–7). The result is displayed in a 2-History Diagram (Fig. 7). In order to compare to different glaciers, a till deposited from the thinnest, recent glacier studied was chosen as an example of a very low degree of processed till, i.e., the Tärna Glacier in Västerbotten County, Sweden (Molén, 2014). This glacier was probably no more than *c.* 10–30 m thick at the place where this till was deposited, and such a small glacier will not impose large forces on the grains (Figs. 2G-H). With this comparison, evidence of even a very thin Dwyka glacier could be detected. Comparison was also made to Pleistocene tills which were deposited by large continental glaciers with different substrata (Figs. 2E-F), Precambrian magmatic/metamorphic shield in Västerbotten and mainly a sedimentary Palaeozoic substratum in Southern Ontario, Canada (Fig. 3B; Molén, 2014).

In Figure 7 the result of the documentation of surface microtextures from the Dwyka Group diamictites for the group A1/SP1 are in one group,
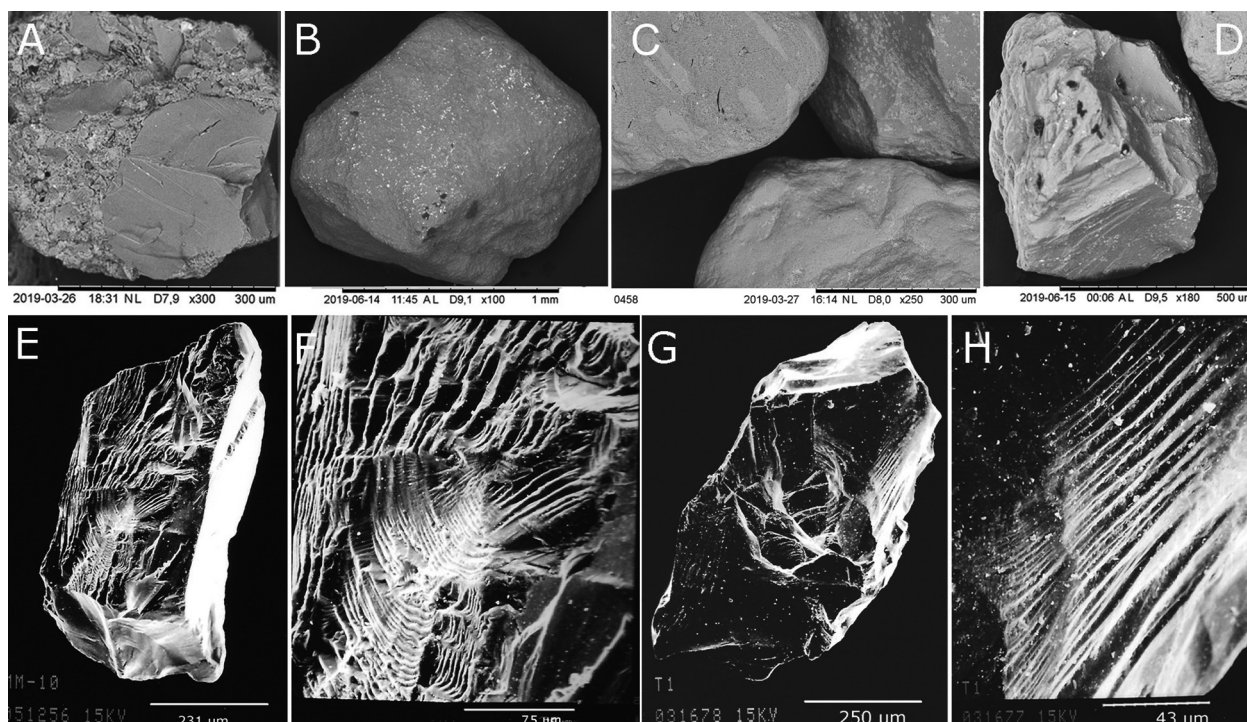

Fig. 2. A-D, Dwyka Group. E-H, Quaternary tills, Sweden (Molén, 2014). **A –** Three quartz grains embedded in silt and clay, similar to all samples from the Dwyka Group (sample F4, a conglomerate). The grains are already fractured inside compact and lithified clay, which makes it likely that the fractures originated during transport and deposition in the conglomerate; **B –** A typical grain from the Dwyka diamictite samples. These grains are commonly regularly abraded and weathered (A1/SP1), and many have been fractured prior to abrasion/weathering, i.e., the grains may display F2 or f2. Grain is classified as A1, SP1, f2 (sample C3a, Nooitgedacht); **C –** Closeup of three typical Dwyka Group grains (sample O2, Denny Dalton). All grains display A1/SP1. The upper two grains also display F2. **D –** Sample G2b, from the site that was interpreted by Visser (1996) to have formed in front of a grounded marine ice sheet. This quartz grain displays the most general overall similarities to a glaciogenic grain, of all quartz grains in the present study. The original appearance of this grain was probably multicyclical. The grain was later heavily fractured. The fractures have been subsequently weathered and regularly abraded, i.e., the fractures have not been abraded much in one place and little or not at all in other places (i.e., they are not irregularly abraded), but there is evidence of regular/'soft' abrasion and weathering all over the grain. Grain is classified as A1, SP1, F2; **E –** Example of a quartz grain from Pleistocene waterlain till, from an area of magmatic/metamorphic bedrock substratum, Sweden. The appearance of the grains from this site is very different in comparison to that of all South African grains, including the grains from sample G which have been interpreted to be rainout till in front of a grounded marine ice sheet (Visser, 1996) (e.g., Figs. 2D and 5). The grain in the picture is heavily fractured and irregularly abraded; **F –** Closeup of the grain in picture E which shows that the white areas of the fractures, in the centre and lower left, are more abraded than the other fractures; **G –** A grain from Tärna glacier, Sweden, a thin Neoglacial glacier. This grain is heavily fractured and irregularly abraded unlike all Dwyka grains; **H –** Closeup of grain in picture G which shows that fractures have been irregularly abraded, as is typical of glaciogenic grains. But, as this glacier is very thin, there is not much abrasion on the grains from this area.
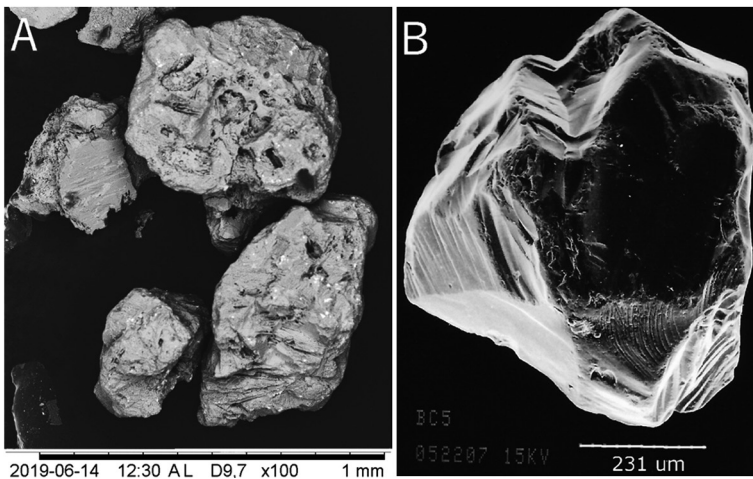
Fig. 3. A – Sample C4m, the thin dark sedimentary layer between the diamictite and the striated pavement. All four quartz grains are heavily weathered. One grain displays a large fracture which is classified as F1 (upper left grain); **B –** Grain from Pleistocene till in southern Ontario (Molén, 2014). The source area for this till is similar to much of the source material of the Dwyka diamictites, i.e., a substratum of multicyclical sedimentary rocks or sediment. This grain is heavily fractured, but the general outline of a multicyclical grain is still evident. The abrasion is strong and irregular, i.e., not the same on all surfaces, as is typical of glaciogenic grains. Classification is F1/A1.
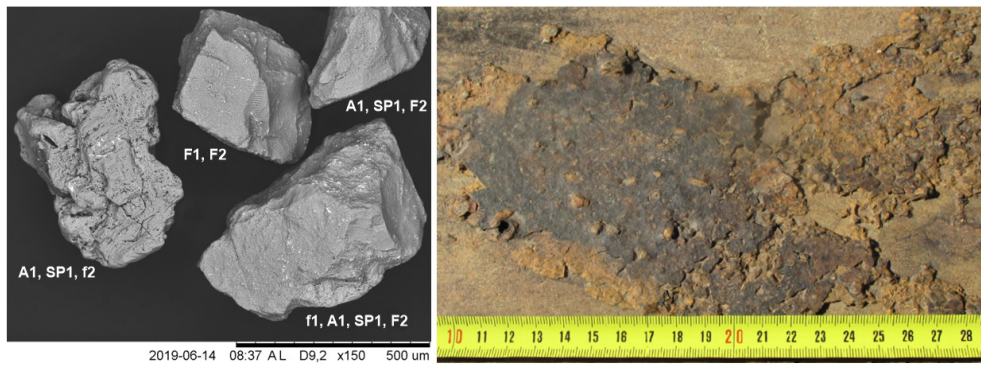

Fig. 4. Quartz grains from sample C-1-1 from the thin, blackened by weathering, diamictite crust directly on top of the Ventersdorp lava, Nooitgedacht pavement (right photograph). The quartz grains are labelled with the identified surface microtextures. The grain on the left is similar to many of the quartz grains from the thin dark sediment between the diamictite and the pavement (sample C4m, Fig. 3A). The two grains to the right are more or less fractured and rounded and display the most common surface microtextures A1/SP1, combined with other surface microtextures. The middle upper grain only displays fractures, which in larger magnification could be sorted into older and more recent fractures. No grain shows irregularly abraded fractures that are typical of glaciogenic grains. There are only fractures which have been regularly abraded, or not abraded at all, and weathered grains (i.e., multicyclical grains, most recent history is A1/SP1).
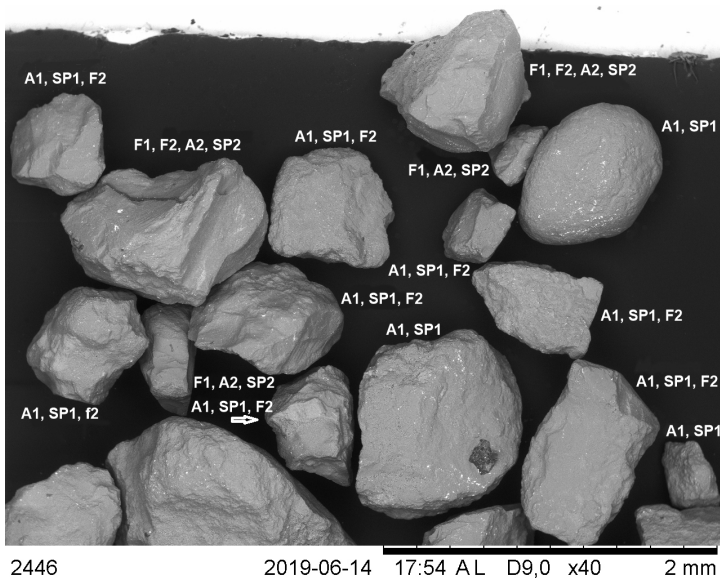

Fig. 5. Sample G1a, "deposited in front of a grounded marine ice sheet" (Visser, 1996, p. 285). These grains are very different from, for instance, Pleistocene waterlain till from Scandinavia (Figs. 2E-F; Molén, 2014). Some grains are almost spherical, and none display the typical glaciogenic appearance of fractures that have been irregularly abraded. If the grains are fractured, the fractures are either solely sharp or otherwise more or less regularly rounded all over their edges, i.e., display regular abrasion which is common in, for example, aqueous environments, but not formed by glaciers.
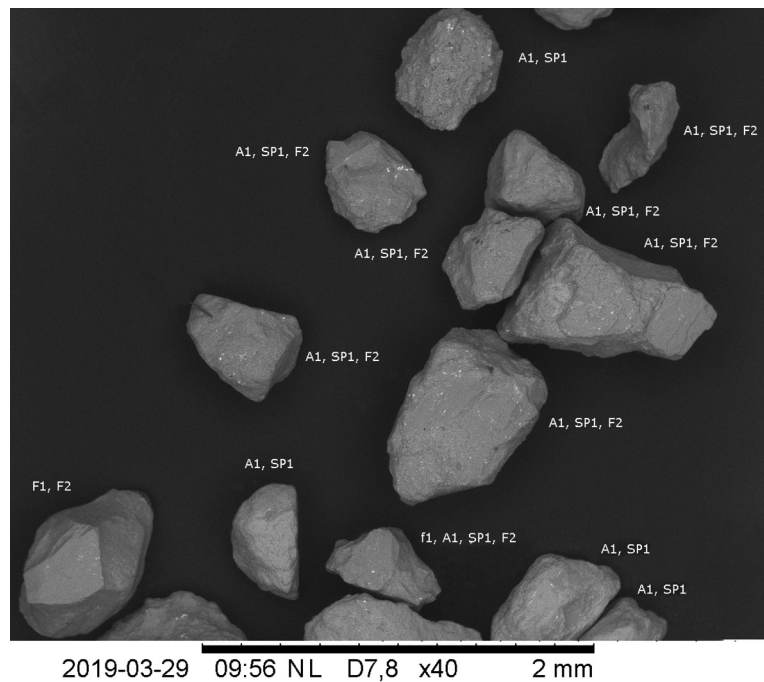
Fig. 6. Grains from sample M2, from Coedmore Quarry, Durban. There are no glaciogenic surface microtextures on any of these grains.

as all samples are almost identical. If the diagrams had displayed a mix of quartz grains from different geological histories, this scatter would blur the diagram, and information would be lost (Molén, 2017). Therefore, all grains with unaltered large fractures (F1) as the single most recent geological incident,

and no other recent (History-1) surface microtextures like chemically unweathered abrasion (A1) or weathering (SP1), are not included in the diagram that shows all diamictites. More detailed discussions, including examples of photomicrographs, can be found in the Supplemental material.

Fig. 7. A 2-History Diagram displaying all Dwyka Group diamictite grains that do not show unaltered F1. Samples C3bm, C4m, conglomerate (F4:s) and striated surface (L1:s) are not included. Dwyka diamictites (circles) are compared to relevant examples from Pleistocene and modern-day glaciers. Curve marked by triangles is from the smallest glacier studied by ourselves, probably not much more than 10-30 m thick (Tärna Glacier, Neoglacial; see Molén, 2014). Curve marked by squares is from tills deposited by thick Pleistocene glaciers with magmatic/metamorphic bedrock as source rocks, Västerbotten County, Sweden. Star marked curve is from southern Ontario, Canada, Pleistocene glaciation, from tills originating to a large part from sedimentary bedrock. The connecting lines in the diagram are drawn to enhance visibility, as described in Molén (2014). These lines are important, as they indicate the general trend of the different surface microtextures, and therefore easily visualise a distinguishable 'geological signature' of the appearance of each sample. The latter will not show up in a histogram. Typical geological signatures in this diagram are multicyclical (A1/SP1, all diamictites), large glaciers (much F1/A1) and small glacier (less F1/A1). The number of quartz sand grains studied are within parentheses, inside the box.
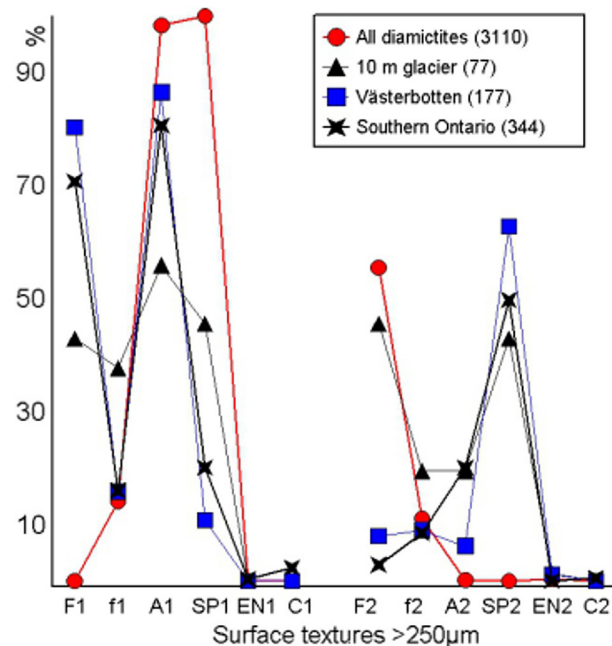
4.2. Pavements

The four striated surfaces/pavements that were studied in the present work display clusters of mainly parallel striations. The only pavement that was covered by a confirmed diamictite was at Nooitgedacht. Iverson (1991) described the appearance of glacial striations as generally short and deflected, due to internal clast movement inside the glaciers. The striations documented here displayed many different appearances.

4.2.1. Nooitgedacht

The pavement area at Nooitgedacht is probably the best known of all pre-Pleistocene pavements in the world. Many small outcrops displaying striated surfaces are exposed in an area of a few thousand square metres (Slater et al., 1932). The striated surfaces are formed on top of Neoarchean Venters-dorp Supergroup andesite lava and are subjacent to diamictites.

The pavements display striations with different appearances in distinct areas. Master (2012) identified three main sets of bearings: 225–232°, 240–256° and 203–216°. But, there is a large variation of bearings, which is partly controlled by small local highs or steep surfaces (Fig. 8A). A more detailed investigation of striations and grooves shows that they are commonly ordered in distinct 'groups' displaying different appearances and bearings. Each group commonly displays internally parallel straight striations (Fig. 8B).

Some areas display striations in so many directions that they appear to be fan shaped. Upon closer inspection, however, they appear to be clusters of parallel striations displaying different bearings, meeting and crossing each other at different points (Fig. 8B).
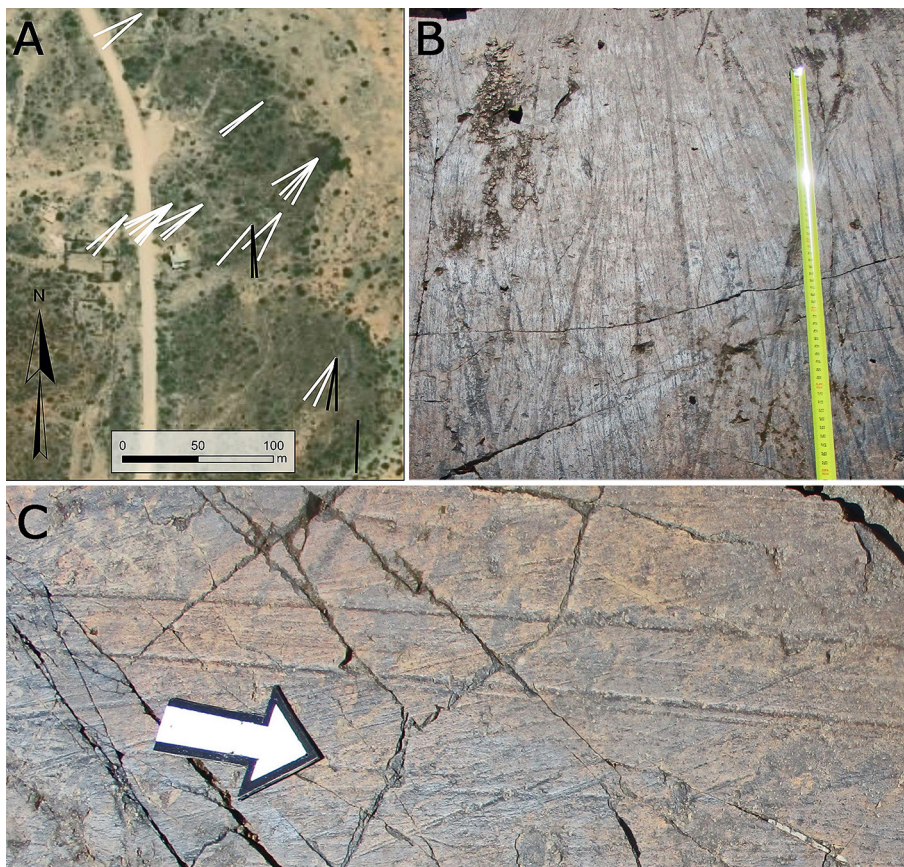

Fig. 8. Nooitgedacht. **A –** Google Earth image displaying the main directions of the striations at different pavement outcrops at Nooitgedacht. The striations which are almost straight south (black lines) were deflected by local highs on steep surfaces. The pavement marked with one black line, in the far south, is photographed in Figures 9B-C, and the one just above, displaying different bearings, is in Figure 9A; **B –** Example from an area displaying thin striations which are commonly less than 1 m long, straight and in parallel groups, which make them appear as regular fans. Note that the striations are criss-crossing, forming almost a conjugate pattern. The ruler is 60 cm long; **C –** Two near-parallel grooves, many metres long, that were probably generated by a single clast. Thinner striations cross the grooves. Arrow is 25 cm.
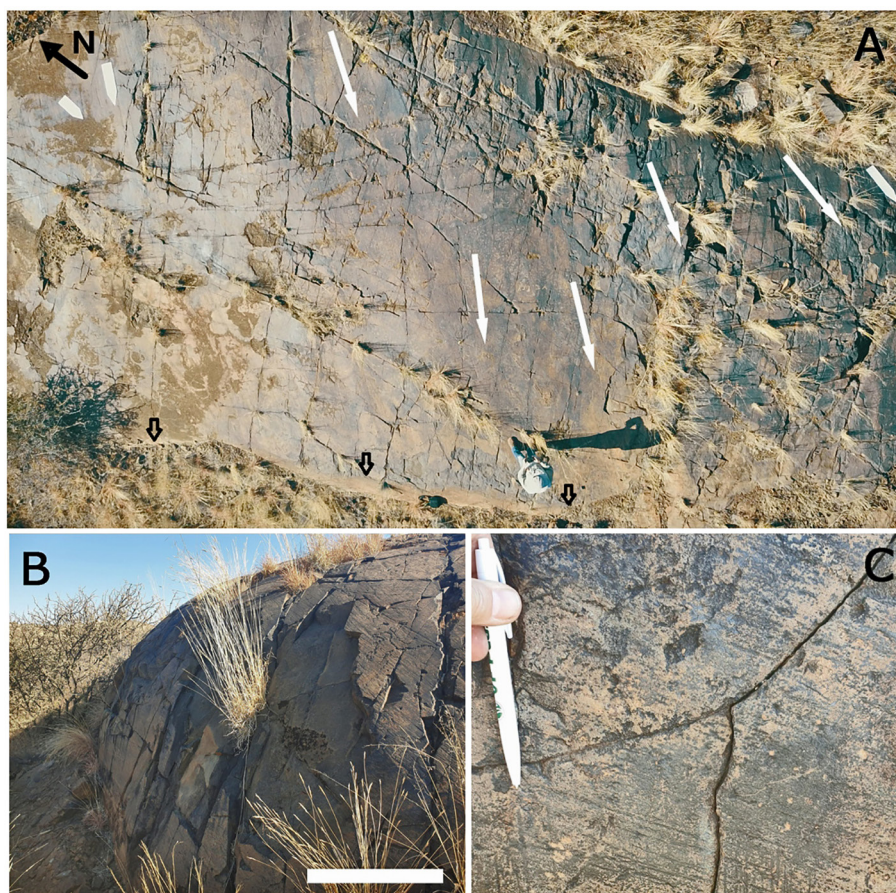
Fig. 9. Nooitgedacht. **A –** Vertical overview of one of many small striated surfaces (see location in Fig. 8A). All white arrows point in the directions of the striations. In the lower part of the photograph, on the lee side edge of the striated surface, there is a small scarp displaying a uniform and steep flat 10-40 cm long slope (marked with small black arrows), down to the next flat level of the outcrop (grass-covered). The appearance of this lee side structure may be interpreted as a cut sheeting joint surface, as there are no large irregularities at this surface. Next to the north arrow and the two small white arrows there is a confined area where the striations are short (approximately four square metres in size; 80% of the striations are <10 cm) and in more varied directions (Supplemental material). Striations at the upper right of the pavement are on a steeper surface and are slightly deflected to be more parallel to the slope of this surface. Those on the near flat surface, higher up on the outcrop, mainly pass straight over and follow the outline of that surface; **B –** This outcrop has a near-vertical wall that is striated horizontally (location marked in Fig. 8A). A large part of the surface is recently exfoliated to a depth of a few cm, following the outline of the volcanic bedrock, with a rugged surface below. Scale is approximately 25 cm; **C –** Closeup of part of Figure 9B. There are 10-20 cm long vertical striations which cross the horizontal striations almost perpendicularly, which shows that there was an intermittent short change in the direction of movement.

The striations are often up to about a metre in length for the thinner ones, and longer for thicker grooves. Deeper striations or grooves are often many metres long (Fig. 8C). Usually these are straight, parallel if two or more are next to each other, but not curvilinear (even if some may show diversions, as is also possible by gravity flow-induced striations).

On steeper surfaces striations are deflected but may still remain more or less parallel (Fig. 9).

In some areas (Fig. 9A) striations are very short, more than 80% may be less than 10 cm long, and only 2% may be longer than 50 cm (100 striations measured; see Supplemental material).

In some places there is a thin veneer-like layer of diamictite material on top of the striated surface which has been moulded into soft-sediment grooves and ridges (Fig. 10).

After removing the diamictite a very thin brown-coloured sediment was evident, which was plastered onto the volcanic striated surface (Fig. 10C). Sedimentary relationships similar to this were also observed at other striated surfaces (e.g., Fig. 11A). This sediment in between the diamictite and the striated volcanic surface was almost totally moulded into small and large ridges and grooves displaying an appearance of striations (Fig. 10C). In the

Fig. 10. Nooitgedacht. **A –** Small moulded sediment ridge which shows 'bouncing' (upper part of picture), then makes a bend and splits into two and later three ridges (compare to similar ridges in Baas et al., 2021, fig. 16); **B –** Grooves and ridges moulded in diamictite on top of the Nooitgedacht striated surface. These are no striations on the bedrock but grooves smeared internally inside the diamictite, on top of the bedrock. Scale lines are in mm; **C –** After removing a part of the diamictite it became apparent that there is a thin sediment plastered onto the lava. This brown sediment (left) is made of internal striations/grooves/mouldings covering the complete surface in the sediment, and are not striations on bedrock. This sediment had disappeared quickly by weathering, so just outside of the diamictite there was only a very thin blackened sediment surface with few striations/grooves/mouldings left (middle). Where the black sediment cover had weathered away, the Ventersdorp lava was at the surface and displayed only a few shallow striations (right).

area just outside of the diamictite cover, the brown sediment had turned black by weathering and had been partly removed by weathering/erosion, and there is only a very thin dark/black sediment left with few of the striations from the brown sediment preserved. Furthermore, where the black sediment had weathered away, the volcanic basement surface displayed even fewer and less deep striations than on the black sediment surface (Fig. 10C). In conclusion, most of the striations and grooves were only present as soft moulded sediment, and only a few of these passed through the sediments and down onto the volcanic basement pavement.

At one site, striations on Ventersdorp lava continued as soft-sediment striations on a diamictite surface on the same plane (Fig. 11A).

In a few areas no striations were recorded, or they were very thin. Some of these areas appeared to be small bypass zones as observed in sediment gravity flows (Fig. 11B) (Cardona et al., 2020; Peakall et al., 2020).

The thin veneer of sediment between the striated surface and the diamictite was mentioned by Slater et al. (1932; see also Visser & Loock (1988) and Visser (1988), who described similar sediments in the near vicinity). The thickness varies between 1 and 10 mm (Figs. 10, 11A). The sediment display strati-

fication on a mm-scale, similar to the superimposed diamictite (Table 1). The thinner dark lower layers (e.g., sample C4m, Fig. 3A, but also partly sample C-1-1, Fig. 4) contain quartz grains which apparently came from a highly weathered area, possibly a former saprolite.

The volcanic bedrock at Nooitgedacht often displays stoss sides that are steep and lee sides that are gentle, as opposed to roches moutonnées, but were labelled drumlinoid complexes by Visser (1988) and Visser & Loock (1988). At the lee sides there is often a short and steep flat regular scarp surface sloping down to a lower level of the volcanic bedrock displaying approximately the same angle (Figs. 9A, 11). At a few places more than one small scarp is present, with a flat surface between (Fig. 11B). The flat scarp surfaces are in some places striated. These regular structures display an appearance that is similar to cut sheeting joints. At one place striations in the bedrock continued to a diamictite surface that displays soft-sediment striations (Fig. 11A).

The volcanic basement bedrock frequently display recent exfoliation in cm-thick layers, both on horizontal surfaces and inclined surfaces, following the surface of the outcrops (Figs. 9B, 11B). There is no evidence of strong unbound glacial abrasion.
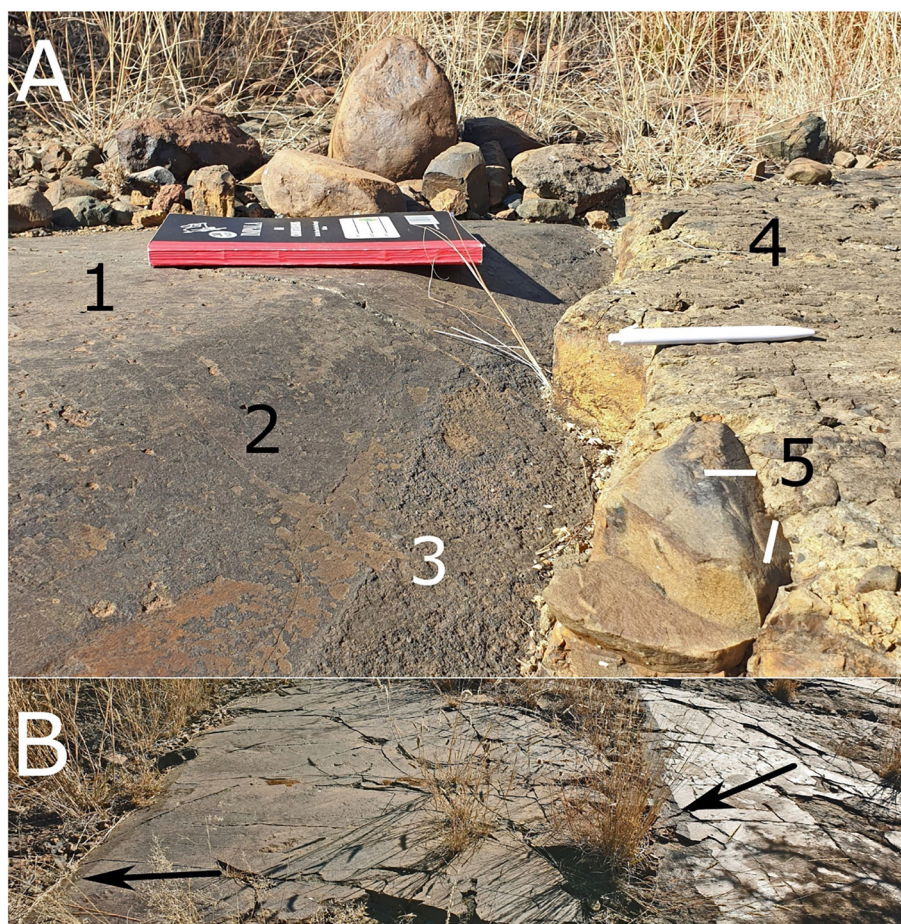
Fig. 11. A – A flat surface of the Ventersdorp lava with striations (1), displaying a joint-like lee-side similar to many other lee-sides of the pavement area (2), a thin veneer-like layer of sediment below the diamictite (compare Fig. 10C) (3), a diamictite with soft-sediment striations at the same level as on the flat lava surface (4) and a boulder with striations in many different directions (two more pronounced striations are marked with thin lines) (5). The striations on the bedrock and diamictite are in the direction of the pen; **B –** This small striated surface displays two long, but low straight-edged joint-like scarps (at the tips of the arrows). On the flat surface between the scarps there are few striations, except next to the left small scarp, and this flat surface therefore may be referred to as a small bypass zone. The general direction of the striations is marked with the long arrows, but both surfaces display groups of striations with different bearings, slightly similar to those shown in Figure 8B.

4.2.2. Douglas

At Douglas there is a pavement displaying grooves and striations on Ventersdorp volcanic bedrock (Fig. 12). The striated surface is approximately 9,000 m^2 in size (Stratten & Humphreys, 1974). Large grooves can be followed for tens of metres. These grooves are commonly a few centimetres deep and tens of centimetres wide. They display a pattern with the appearance of a washboard, and becomes deeper towards the green area of Figure 12A which is marked with arrows and shown in Figure 12B. Both striations and grooves are very long and parallel. They display no unequivocal evidence of the variety of glacial features that prevail on Pleistocene pavements, like deviations from a parallel path, and moving vertically and horizontally inside a gla-

cier-produced curvilinear path (Figs. 12B-C). There is no diamictite in the area, but there is shale nearby, with sparse outsized clasts up to 3 cm long. This shale is often interpreted to be postglacial or late glacial Ecca Group (Stratten & Humphreys, 1974).

4.2.3. Oorlogskloof

At Oorlogskloof there is a soft-sediment sandstone pavement which is covered by sediments made up of sand containing little clay and a few outsized clasts. The pavement area is slightly higher compared to the surroundings, except for a quadrangle stretching from slightly north of the pavement and to the west. The covering sediments have been defined as sandstone or pebbly sandstone (Cape Geosites, 2014). The underlying striated sandstone
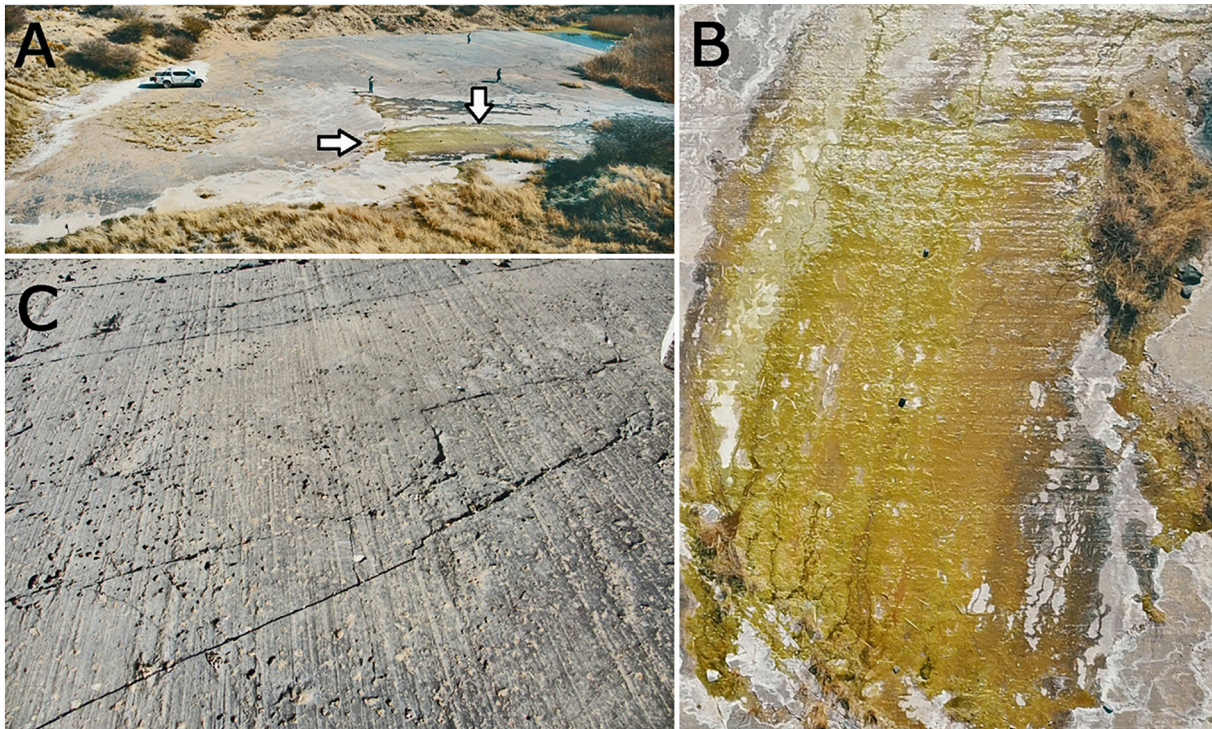
Fig. 12. Douglas pavement. **A –** Overview. The area marked with arrows is displayed in B; **B –** This area displays large parallel grooves forming a washboard pattern. Vegetation grows in the deeper parts of the grooves. Depth difference from top to bottom of grooves is less than 10 cm and commonly only a few cm; **C –** Closeup of a section with only thin grooves and striations. The parallel direction of striations and grooves is clearly visible. The lower part of this photograph is about 1 m across.

surface contains similar outsized clasts as the sandstone covering the pavement. There is no diamictite in the near surroundings.

The pavement is striated, grooved and fluted parallel (Le Heron et al., 2019) in soft sand (Fig. 13). Four stacked levels of striated surfaces were recorded (Fig. 14B). The most outstanding structures in the pavement are parallel long stretched furrows and ridges which are V-shaped in appearance, with steeper north sides than south sides, the latter displaying grain flow lobes (Fig. 13B). The furrows and ridges have been interpreted as glaciogenic flutes by Le Heron et al. (2019). Three of these ridges are especially outstanding (Fig. 13C). The grain flow lobes on the south side are slightly deflected in the flow direction (Fig. 13B). The steeper north sides are more like a flat wall, molded and planed off, and therefore are more compressed and cemented with an appearance of clay smear (Vrolijk et al., 2016). In some areas, this steep surface is slightly vertically 'ribbed', i.e., with an appearance that is similar to vertical slip surfaces of many faults. Single or occasionally multiple tool marks in different directions, comparable to the size of pebbles in the overlying sandstone, have been imprinted onto the elongated forms (Fig. 13B).

There are a few fractures or joints which are perpendicular to the direction of the striations and grooves in the pavement, and in places next to where the pavement shows slight vertical movement (Fig. 13A). The sandstone covering the pavement area was deposited in an east-west path, like large sand lobes, in the same direction as the striations. The sand flowed upgradient while coming up from below of the pavement surface from the east, then covered, thrust and squeezed parts of the pavement (Fig. 13A, at number 4, and Fig. 14A). The sedimentary structures in the sandstone display upward movement during deposition over the pavement area, at the north side (Fig. 13A, number 3). These sand lobes are similar to sandy debris flow lobes. A large sand lobe at the east side of the striated surface deflected and warped the underlying pavement so that all furrows and striations have been remoulded and in part obliterated (Fig. 14A). All data show that the pavement and the underlying sedimentary section were soft, probably in a semiplastic or apparent cohesion condition, during the whole depositional event.

Stratigraphically, above the pavement area are convex streamlined 'sand bars', the largest one more than 10 m long and 1 m high. The largest 'sand bar'
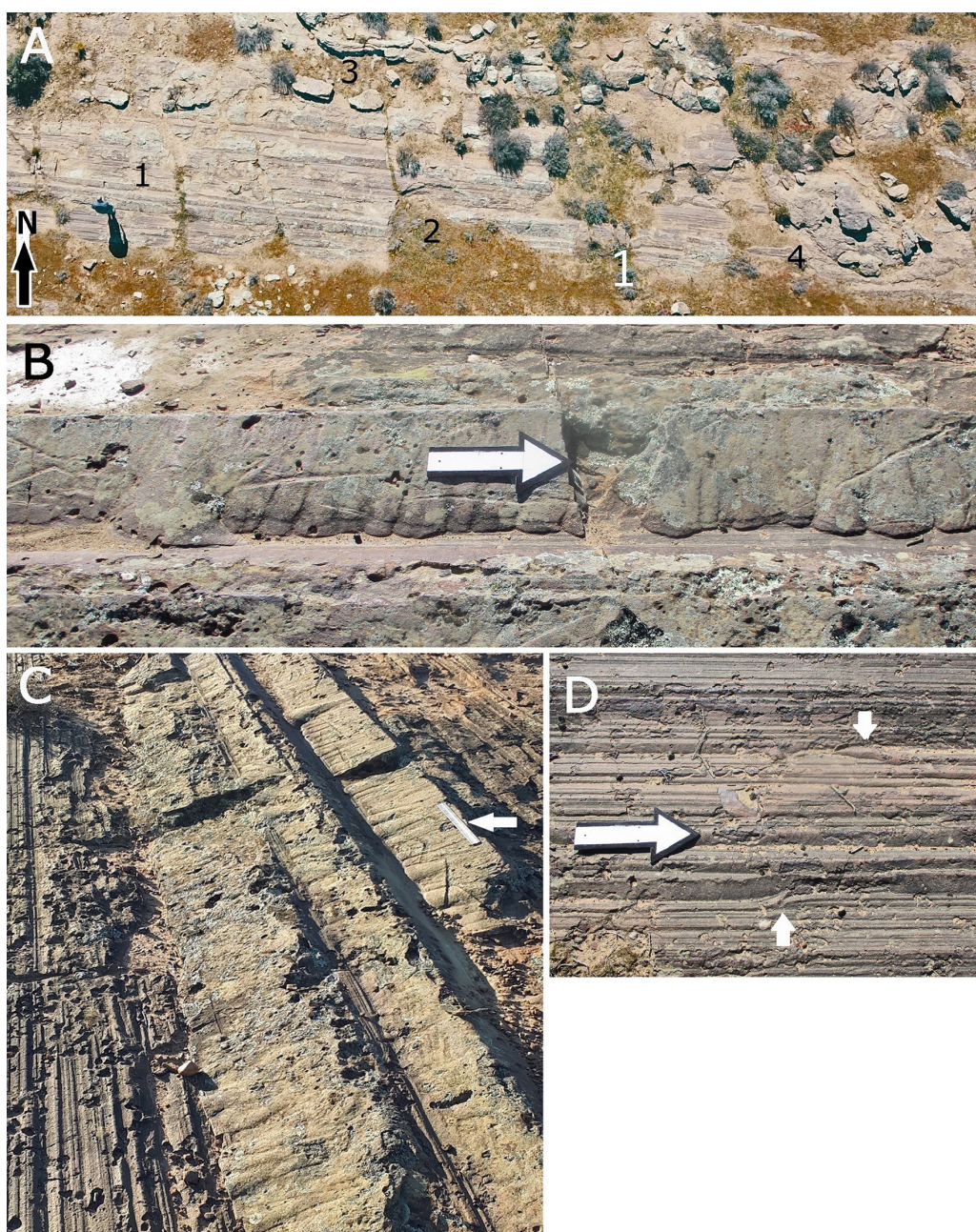
Fig. 13. Oorlogskloof. **A –** Vertical overview of part of the pavement (person for scale). The surface of the striated surface is higher than the surroundings, except on the western and parts of the northern side. Parallel furrows and ridges are visible over most part of the photograph, marked at two places with the number 1. Some furrows are slightly soft tectonically bent. There are a few fractures in the pavement area which are perpendicular to the furrows. At number 2 the pavement is lowered on the right side of one perpendicular fracture (pavement is partly covered with grass). Sediments continue in a path up from the lower areas (from the north and east) and cover the pavement, and there are bedding planes in the sandstone in these overlying sediments (above numbers 3-4); **B –** Details of part of the area that displays small sand lobes, showing that these flowed down onto and covered parts of the striated and grooved surface at the bottom of the V-shaped depressions. The grain flow lobes are slightly deflected in the flow direction, i.e., to the west (opposite to the direction of the arrow), which is more evident on the left side of the arrow. Straight or curved shorter single grooves pointing in different directions are superposed onto the grain flow lobes; **C –** The three most outstanding parallel elongated furrows/flutes which display sand grain flow lobes. Photograph taken in front of person in Figure 13A. The ruler in front of the arrow is 30 cm; **D –** Closeup of pavement. Note that one groove makes a short bent 'jump' (lower small arrow) and one groove is deflected and then moulded together with the underlying one (upper small arrow), which indicates rotation of the tools making the marks. Flow direction is opposite to the arrow. Large white arrow is 25 cm.
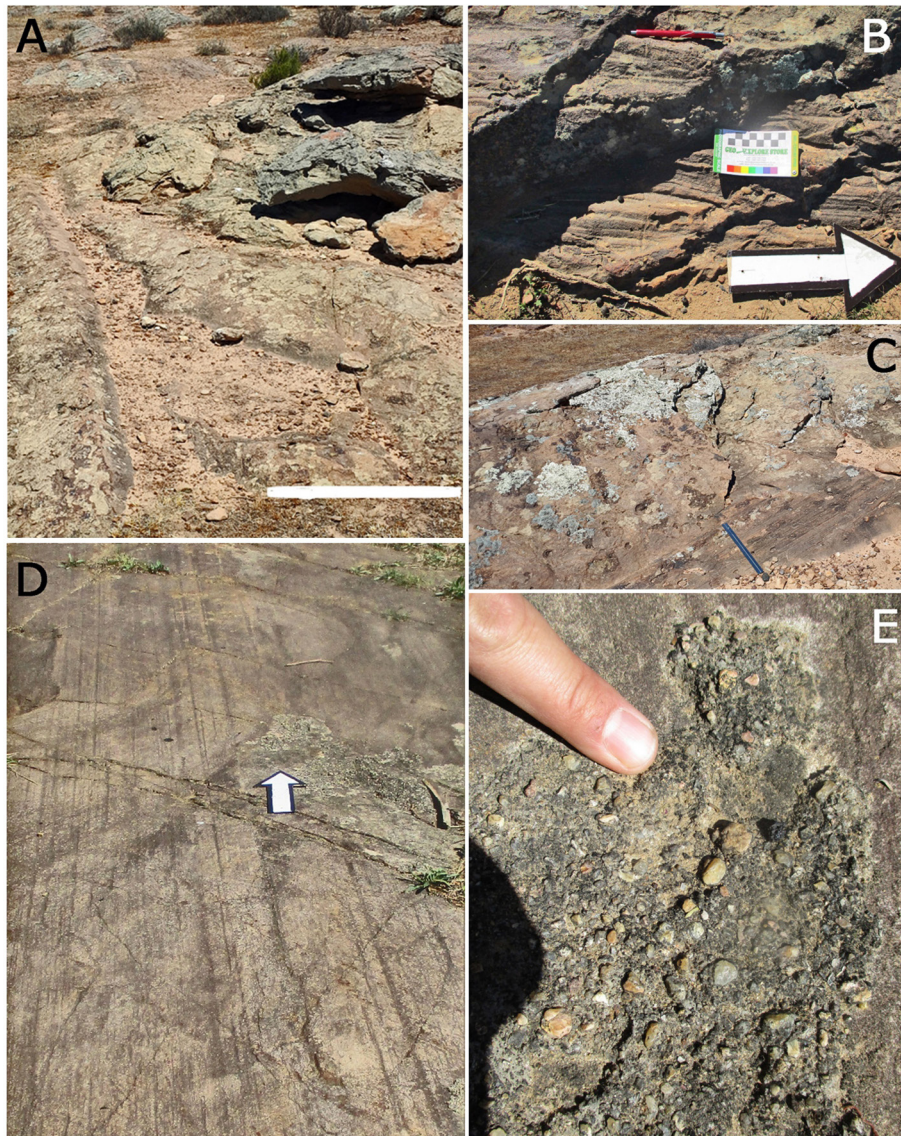
Fig. 14. A-C – Oorlogskloof, D, E – University of KwaZulu-Natal, Westville Campus, Durban. **A –** A large stratified sand lobe, with bedding planes, has deflected and remoulded the sandstone of the striated surface a few metres, the latter of which must have been in an apparent cohesion or semiplastic condition. Sand lobe is visible in Figure 13A, above and to the east of number 4. White marker is *c.* 1 m; **B –** Four stacked soft-sediment striated pavements, i.e., this is the internal structure of the sandstone in this area; **C –** Internal part of the large flute, displaying bedding planes similar to the sandstone which covers the pavement in Figure 13A (numbers 3-4). The ruler is 30 cm; **D –** Striations on the sandstone surface are long and parallel; **E –** Small area on top of the striated surface in D, displaying a thin veneer of sand and gravel (sample L1c). Arrow is 25 cm.

was described as a glaciogenic flute by Le Heron et al. (2019). This bedform consists of sand, partly conformable and following the surface of the 'sand bar', with the internal composition displaying bedding (Fig. 14C). Some smaller streamlined convex 'sand bars' next to the largest one are partly descending below the base level of the pavement surface.

4.2.4. Durban

At Durban's University of KwaZulu-Natal Westville Campus there is a pavement of approximate-ly 100 m² on sandstone, and similar soft-sediment pavements are in a zone around Durban (Bangert & Von Brunn, 2001; Haldorsen et al., 2001). No confirmed diamictite is present. Striations and grooves on the pavement are long and parallel but not curvilinear (Fig. 14D). The longest striation is 6 m. On top of the pavement, there are small veneers of mainly sand and gravel (Fig. 14E). A sample of a sliver of sand and gravel on top of the pavement was studied by SEM (sample L1c; Supplemental material).

5. Discussion

5.1. General geology – Dwyka Group

The sediments of the Dwyka diamictites commonly are devoid of large sand grains. All diamictite matrix sediments appear to be mud in which grains from different environments have mixed, mainly multicyclical grains but some that could have been incorporated more directly from bedrock.

Many diamictites are stratified on a large scale, but some diamictite subsamples display stratification on a mm-scale (Table 1). Most samples were small (usually <5x5x3 cm), so stratification was unexpected, and internal structures were not looked for.

At site H, Elandsvlei farm area (Blignault & Theron, 2015), an abundance of brown diamictite blocks within grey diamictite were documented (Fig. 15). These were transported and slid into position, as there are flow structures in the grey diamictite around the brown diamictite blocks. This also indicates that the lower grey diamictite was in a soft condition. Sediment gravity flows commonly pick up and transport intact weathered rocks, soft sediments, including aggregates of boulders and sediment gravity flow deposits, even with intact stra-
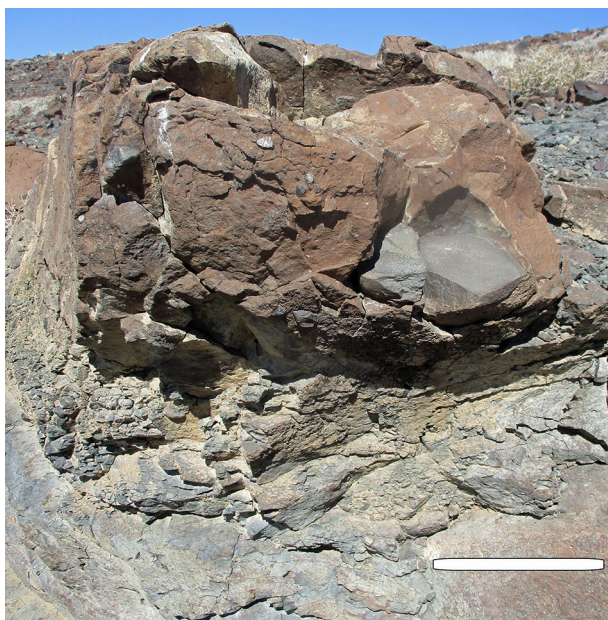

Fig. 15. Many brown aggregates of diamictite boulders were inside the grey diamictite at site H, Elandsvlei farm area, with flow or load structures in the grey diamictite around these boulders. It was evident that the brown boulders slid into place. The grey diamictite apparently was in a soft and wet condition during deposition of the brown aggregates. White line is *c*. 1 m long.

tigraphy, without disintegrating them (Schneider & Fisher, 1998; Major et al., 2005).

5.2. SEM studies

5.2.1. Origin of surface microtextures and SEM study

There is nothing unusual about the appearance of the surface microtextures studied from South Africa, but similar surface microtextures are present in Quaternary samples from non-glaciogenic environments (Mahaney, 2002). There is no evidence of coatings detected during SEM analysis, and the surface microtextures on the quartz grains are indisputable (compare Somelar et al., 2018). The main difference between the South African samples and Quaternary glaciogenic samples is the combinations of surface microtextures. The typical glaciogenic combination of fractures that are irregularly abraded are not present on any quartz grain of the South African samples.

5.2.2. General surface microtextures on quartz grains

Figure 7 shows combinations of surface microtextures from Dwyka diamictites, which are different from, and actually in their details contrary in apperance to, surface microtextures displayed by glaciogenic grains. No grain from any sample displays large fractures and irregular abrasion, i.e., the combination F1/A1 typical of glaciogenic grains. The samples display an almost 100% occurrence of A1/SP1 and small and/or older fractures (f1, F2, f2) (examples in Figs. 2–6). Furthermore, minute surface microtextures on grains from sandstone that has been interpreted as a glacially reworked sediment by Le Heron et al. (2020), do not display any glaciogenic features.

When investigating the possible impact on the surface microtextures from post-depositional processes in the field and laboratory methods, there is no evidence of any modification of the results, except in some probably low degree for the origin of History-1 fractures/F1 (Supplemental material). No History-1 fractures (independent of their origin) in the samples show a resemblance to glaciogenic surface microtextures, but all studied grains display original A1/SP1 followed by single unaltered F1-fractures. Hence, the F1 then reclassifies the older geological history of A1/SP1 to A2/SP2. There was no evidence of almost simultaneous F1/A1 (irregular A1), as is the combination of surface microtextures which is generated by glaciers. A few grains displayed minute surface microtextures that

often are present in glaciogenic material, like conchoidal fractures (Mahaney, 2002); however, these minute surface microtextures do originate in any high-energy environment and not only by glaciation. In the South African samples these fractures show either no abrasion or only regular abrasion caused by long-time exposure to flowing water (Molén, 2014). The samples contain a mix of grains which would be expected from non-glacial processes, such as tsunamis, mass wasting and sediment gravity flows (e.g., Mahaney, 2002; Molén, 2017; Costa et al., 2019). Surface microtextures typical of glaciated areas, i.e., F1/A1, are absent from the Dwyka samples, and there is no evidence of obliterated F1/A1 surface microtextures in any sample.

It would be exceptional if no grain from any diamicitite sampled showed evidence of glaciation. Surface microtextures can be different or change, if transported with water, in periglacial areas, or if all samples are from supraglacial/englacial sediments, but there was no evidence of such environments from surface microtextures or macrotextures in the Dwyka Group diamictites (Mahaney, 2002; Molén, 2014, 2017; Kalińska-Nartiša et al., 2017; Kut et al., 2021; Passchier et al., 2021; Górska et al., 2022; Kalińska et al., 2022). All diamictite samples are compressed and they do not show geological features of any other environments than those that would be interpreted as tills or debrites.

A further observation is that the southern samples (C-J) show 44–57% F2, compared to 48–70% for the northern samples (K-Q) (Table 1). This may indicate that grains from the south were transported over a longer distance, as they are more rounded and therefore display less F2. Samples from the northern sites display more protuberances which indicate sedimentary source rocks consisting of little-rounded grains or magmatic/metamorphic source rocks (Molén, 2014). The rounding of the grains is not glaciogenic but only created from less energetic environments where a combination of regular mechanical abrasion and slight chemical surface weathering are the most common processes (Molén, 2014).

5.3. SEM – detailed discussion of results

The diamictite at Nooitgedacht is of special interest because it is situated directly on top of a striated surface and displays mainly surface microtextures A1/SP1. The rarely reported thin sedimentary veneer-like layer between the pavement and the diamictite is present in many areas (Figs. 10, 11A). This thin sedimentary layer displays no large dif-

ferences in surface microtextures compared to the diamictite, except that there is more abrasion in a thicker brown bed (sample C3bm) and less in a thinner dark bed (sample C4m) (Figs. 3A, 10, 11A). Even if the thicker brown sediment (sample C3bm) was clearly deposited by a more fluid process than the overlying diamictite, it still is mostly in the clay, silt and fine sand sizes, and cannot have been transported over a long distance apart from the overlying diamictite. The thinner dark sample C4m appears to be a mix of transported grains (i.e., surface mictrotextures A1/SP1), similar to all other diamictites from the Dwyka Group, and heavily weathered quartz grains displaying no surface microtextures indicating transport (e.g., no A1), but heavy weathering (SP1) indicating grains released from a possible saprolite. Sample C4m displays less A1, much less F2 and is much more weathered than other grains from Nooitgedacht (Fig. 3A; Supplemental material). The high degree of weathering explain the absence of F2 on many C4m-grains. The documentation of surface microtextures shows that there is commonly a single history of fracturing of sample C4m, either F1 or F2, which could also indicate that F1-grains from this sample may have been fractured during the preparation work because they were heavily weathered. Slight weathering in some cases may create more rounded forms that can be mistaken for abrasion, and therefore the recorded abrasion surface microtextures (A1) may be slightly overestimated (Molén, 2014). The thin sedimentary beds in samples C3bm and C4m correspond to traction carpets, a common structure in the lowermost part of sediment gravity flows, but not below till (Talling et al., 2012; Peakall et al., 2020).

Diamictites subsampled at sites F-Q display similar macrofeatures as have earlier been interpreted to be glaciogenic by previous researchers (Table 1, examples in Figs. 2–6). Sample G diamictite has been interpreted by Visser (1996) to have formed in front of a grounded marine ice sheet, but the surface microtextures are similar to all other diamictite samples, displaying the non-glaciogenic combination of A1/SP1 (Figs. 2D, 5). The difference in surface microtextures is clear when compared to grains from confirmed glacial deposits (Molén, 2014; Figs. 2E-F). None of the grains analysed in any sample showed the typical surface microtexture combinations associated with glaciation. Grains from sediments similar to the sandstone pavement at Durban (L-samples), inside of the conglomerate (F4-samples), and from weathered granite (small fragments of weathered granite, *c.* 2x1x0.5 cm, were present in samples P1a, P3b and P5b) have probably contributed to these diamictites (these grains display

mainly the same basic appearance and surface microtextures; see Supplemental material).

Even very small glaciers rapidly generate large numbers of glaciogenic surface microtextures (Molén, 2014), and there is no evidence of glaciogenic surface microtextures in any of the Dwyka diamictite samples (compare to tills from any Pleistocene and more recent glaciers, Figs. 2–7; Mahaney, 2002; Molén, 2014, 2017).

5.4. Pavements/striated surfaces

The pavements of the Dwyka Group display various features that are commonly associated with basal shear zones of submarine mass flows. The striations and grooves in the four striated surfaces studied do not display continual short-distance variations, neither vertical nor horizontal deflections, similar to how these form by clasts which are frozen into ice (Iverson, 1991). Even if glaciers were cold based, displaying none or almost no movement, a clast at the bottom is never frozen with no minute internal movement within the ice. This is as opposed to clasts in dense sediment gravity flows or slides where the process is so fast that clasts may move in a straighter manner, i.e., hundreds of metres in seconds or minutes (Piper et al., 1999; Peakall et al., 2020). But, sediment gravity flow striations and grooves may also be short and curved.

5.4.1. Nooitgedacht pavement
The striations at Nooitgedacht display many different bearings, but are mostly internally straight and ordered in generally parallel patterns. The striations are also grouped, deflected and differ in appearance between various confined areas. These appearances, including 'conjoining' and crossing striations, are consistent with sediment gravity flow mechanisms (Draganits et al., 2008, fig. 11), including flow diversion in an expanding current or flow (Potter & Pettijohn, 1963). The small area which displays perpendicular vertical striations could be interpreted to have formed by a boulder that suddenly settled under gravity after slowing to below the critical velocity of the flow (Fig. 9C). The areas with soft sediment-moulded striations or grooves plastered onto the Ventersdorp lava, but with few striations below the sedimentary rock, indicate that it was not a thick glacier that was responsible for the striations. This evidence of striations and moulds in soft sediments, which were not transferred onto the bedrock below, indicates a process by which sediment masses passed with only little downward pressure (Fig. 10C). Furthermore, this evidence is at odds with an

interpretation that weathering of the underlying bedrock dissolved most of these tool marks after their formation, as an explanation of the decrease in both number and depth of striations and grooves. Areas with no striations on the Ventersdorp lava could then be classified as small bypass zones, since a large glacier would impact the overall bedrock more overall but with local variations in abrasion and plucking. And clasts within a glacier would always randomly change their vertical and horizontal directions, not commonly producing straight and invariable sub-parallel or parallel tool marks, but almost always constantly asymmetrical tool marks. The full spectrum of striations and grooves at Nooitegedacht, i.e., the grouping, the parallelism and the minute appearance of the striations and grooves, are consistent with and indicative of sediment gravity flow origins. Striations and grooves on hard basement rocks in the northeast of South Africa appear similar to those at Nooitgedacht, but these are covered by stratified diamictite which is interpreted as sediment gravity flow deposits (Dietrich & Hofmann, 2019).

Thin basal beds of sediments, i.e., traction carpets, are common below cohesive debris flows, and are similar to the thin sediment beds below the Nooitgedacht diamictites, but are not displayed by glaciogenic deposits. Soft sedimentary deposits are easily eroded away by glaciers except in more confined and shielded areas. The mm-thick dark layer (sample C4m), which we interpret as part of a traction carpet, contains a mix of highly weathered grains displaying no or little evidence of long transport, from a possible saprolite, and grains rounded from a long time of low-energy impact which may be interpreted as from long-distance transport (Mahaney, 2002; Molén 2014, 2017). The thicker brown layer of sediment below the diamicite also resembles a traction carpet, and displays mostly far-transported grains (i.e., sample C3bm).

The smooth Ventersdorp lava surface below the diamictites is commonly exfoliated, displaying rugged surfaces beneath (Figs. 9B, 11B). There is evidence of slight erosion on top of the lava but no evidence of strong glacial abrasion, which would in at least the more outstanding/steep areas cut deeply into and bevel the bedrock surface straight through any former weakness planes. Furthermore, the pavement is in an area where the subjacent bedrock is mostly composed of Ventersdorp lava (Van der Westhuizen et al., 2006), but the clasts in the diamictite are composed of a mix of different lithologies and not mainly local lava clasts. The matrix of the diamictite is not composed of much dark material, except in the thin basal sediment layer which

is probably blackened by weathering (sample C4m and partly in sample C-1-1; compare to Figs. 4 and 10B-C), but generally mostly light minerals. This observation enhances the indication that the bedrock was not heavily eroded by a thick glacier, but was only bypassed by sediment gravity flows.

The so-called drumlinoid complexes or roche moutonnées in the area do not display evidence of glacial sculpting, but mostly of weakness planes in the lava which have been only slightly abraded by the process which formed the striations and grooves. The small scarps and the regular and uniform bedrock areas next to these surfaces show no evidence of strong shifting, glacial plucking and irregular abrasion. These features simply display intermittent release of rocks along weakness zones of what appear to be sheet jointing in a more uniform, less erosive and brief process consistent with sediment gravity flows. All these observations are evidence that the general appearance of the bedrock (including possible residues of saprolites) was formed long before deposition of the diamictites, i.e., there is no evidence of strong glacial erosion. The major geomorphological bedrock features of the area may have been inherited from before the deposition of the diamictites.

5.4.2. Douglas pavement
The Douglas pavement is flat and very regular, which could be an argument for a glaciogenic origin. However, even if there had been a very slow moving cold-based glacier, one in which clasts would not move/rotate much inside the ice during transport and come into contact with the underlying surface, one would expect at least some movement in the basal part of the glacier with evidence of this displayed on the pavement. There is no obvious evidence for such movements. In a slide or cohesive debris flow, the material may be transported more or less as one large mass (Peakall et al., 2020), albeit with some internal movement inside the mass. The documented lack of diamictite close to the outcrop is more indicative of natural processes of a debris flow that simply passed through the area without depositing any sediments.

5.4.3. Oorlogskloof pavement
Le Heron et al. (2019) deduced three different episodes of deposition and erosion of sediments at Oorlogskloof as movements of a glacier that was grounded, partly uplifted by the sea, and grounded once more. However, there is no evidence for recurrent vertical movements of a marine glacier (or an iceberg) at Oorlogskloof, as the geological work has been generated mainly sequentially on

the same surface. The erosional events and deposition of new sediments are localised, and there is no evidence of a large glacier. If the parallel long ridge and furrows in the pavement were grooves or flutes made by glaciation, it would require the generation of very similar V-shaped elongated structures, either by a few, near-identical boulders (or iceberg protuberances) moving straight next to each other, or squeezing by a glacier of many flutes next to each other made in the same V-shaped sharp-crested forms with similar inclinations. After the generation of these structures there would have to follow uplift of the glacier and subsequent grain flows on the gentler side of the flutes.

Leaving the glaciogenic interpretation aside, the appearance of the V-shaped flutes displays similarities to joints followed by small faults in the sediment generated by tectonic movement, i.e., faulted joints (Wilkins et al., 2001). Joints in sandstone are commonly straight and may be parallel for long distances (Cruikshank & Aydin, 1995; Loope & Burberry, 2018), and the overall appearance of the V-shaped structures are similar to faulted joints (Wilkins et al., 2001). The subsidence of parts of the pavement area, and the perpendicular fractures, may also have originated during the vertical movement, as there commonly are perpendicular fractures where there are joints.

The exact origin of the streamlined convex flutes superposed on the pavement, the largest described by Le Heron et al. (2019), is unclear (Fig. 14C). The few less prominent but similar forms next to the larger bedform are partly below the base level of the pavement, indicating uplift of the pavement area. These forms partly display the appearance of linear sandbars, sand ridges or small flowbands (Dufresne & Davies, 2009). They are made up of mainly sand, and the flute of Le Heron et al. (2019) displays internal bedding planes. These flutes appear to be from sandstone that in some extent moved upwards, from the lower area next to the pavement, and covering part of the pavement, and are aligned in the same main general direction as the sand covering parts of the pavement (Fig. 13, numbers 3–4).

The striations and grooves at Oorlogskloof display similarities to striations and grooves in sediment gravity flows in many places (Enos, 1969; Peakall et al., 2020), and especially to Neoproterozoic/Lower Cambrian striations and grooves from submarine landslides at the base of superposed sandstone beds in India (Draganits et al., 2008). There are no similarities to any soft-sediment glaciogenic striations and grooves. The appearance is fully consistent with pavements caused by debris flows which leave grooves, striations and short-

er tool marks behind (compare Ortiz-Karpf et al., 2017; Peakall et al., 2020).

The different episodes of deposition and erosion of sediments at Oorlogskloof may be interpreted as evidence of different sediment gravity flows. The sediments covering the pavement display sharp and irregular fronts, similar to sediment gravity flow debris tongues (Shanmugam, 2016). The palaeoflow in the surrounding area is in one main direction and a few lesser 'valley glacier' flow directions (Visser, 1981; Cape Geosites, 2014), similar to what has been observed for more recent large slides/sediment gravity flows (e.g., Haflidason et al., 2004).

5.4.4. Durban

The striated surface at Durban University is small, and the striations are more or less parallel. The small sliver of sediment on top of the striated pavement either was sediment between the pavement and any diamictite, or otherwise a part of a stacked pavement. Nothing on this striated surface makes it necessary to invoke glaciation, and the appearance is more consistent with a sediment gravity flow origin.

6. Conclusions

As briefly described above (Introduction), evidence from palaeochemistry, palaeontology and palaeomagnetism may be ambiguous and do not conclusively support continental glaciation in South Africa during the Late Carboniferous and Early Permian. The Dwyka Group deposits are present in downwarped basins controlled by tectonics; hence, their origin is consistent with a subaqueous fan environment displaying debris flows. This is also supported by the great depth of the overlying Ecca Group shales and sandstone, which show that the downwarping period persisted until after deposition of the diamictites until at least the southern parts of the area became a deep-water basin plain (Brooks et al., 2018; Hansen et al., 2019). This fact shows that the Dwyka Group deposits are different from Pleistocene tills, as the former are deposited in a downwarping area and the latter on a shield. Sediments deposited on top of shields are much more prone to erosion. However, those laid down in synclines often persist and may later turn into positive topographic erosional remnants or mountains. This seems to be evident from the appearance of the local geology, especially in the south of South Africa, where the thickness of the sediments is greatest. In conclusion, if the sediments in the Dwyka Group were glaciogenic, then there are no deposits from former subaqueous fan environments from this

period. This lack of fan deposits is problematic because subaqueous fan environments are very common in modern-day depositional settings, particularly in downwarping basins (Talling et al., 2015, Shanmugam, 2016), and the Dwyka Group diamictites are covered by sediments deposited in a fan environment (Hansen et al., 2019).

The four major cycles of glaciation, interpreted from the sedimentary succession of the southern parts of the Dwyka Group (Visser, 1997; Dietrich & Hofmann, 2019), can be equally well interpreted as four episodes of more or less extensive downwarping and sedimentation. There are no geological inconsistencies which follow from an interpretation of the Dwyka Group as having formed mainly by recurrent flooding and sediment gravity flows of occasionally large magnitude.

The SEM study has demonstrated that not a single quartz sand grain displays the typical glaciogenic combination of surface microtextures, fracturing and (irregular) abrasion (F1/A1), that would have been generated almost simultaneously below a glacier. Except for single F1- or f1-fractures, the grains display more or less surface microtextures that probably originated during release from weathered bedrock (mainly F2, f2, but a few EN2), but most grains display surface microtextures that need a long time to be generated, i.e., regular A1 and SP1 on more or less spherical multicyclical grains (compare Molén, 2014, 2017). Quartz grains transported over a short distance display slightly sharper fractures and protuberances compared to those transported over a long distance (comparing northern and southern samples from the Dwyka diamictites). Finally, there is no evidence of artificial surface microtextures or chemical coatings on the grain surfaces that obscure the original surface microtextures.

The overall appearance of the pavements displays many structures that can be expected to have been generated by sediment gravity flows but not by glaciers, even if some of the striations are not at odds with glaciers and marine ice sheets. This is evident from the appearance of the Nooitgedacht pavement but also from the Durban and Douglas pavements.

The history of formation of the more complex Oorlogskloof pavement area probably was some variation of the following episodes. Details are visible in Figures 13 and 14, but the overview described below is in Figure 16:

1. Tectonically generated sediment gravity flows passed across the area, forming surficial striations and internal hydroplastic slickenside striations in soft sediments.

2. Subsequently, the small striated area was uplifted, or alternatively the area south, east and partly in the north sunk. The long linear V-shaped furrows were formed, first by slight compression and then partly by jointing followed by slight faulting. Clay smearing took place in some areas of the steep sides.

3. During the minor vertical movement, sandy grain flow lobes were formed on the gentle sides of the furrows.

4. Almost simultaneously sandy debris flows pushed and deformed some of these V-shaped forms to smoother forms and also deposited the linear sand structures in the area. Because of apparent cohesion or semiplastic condition in the
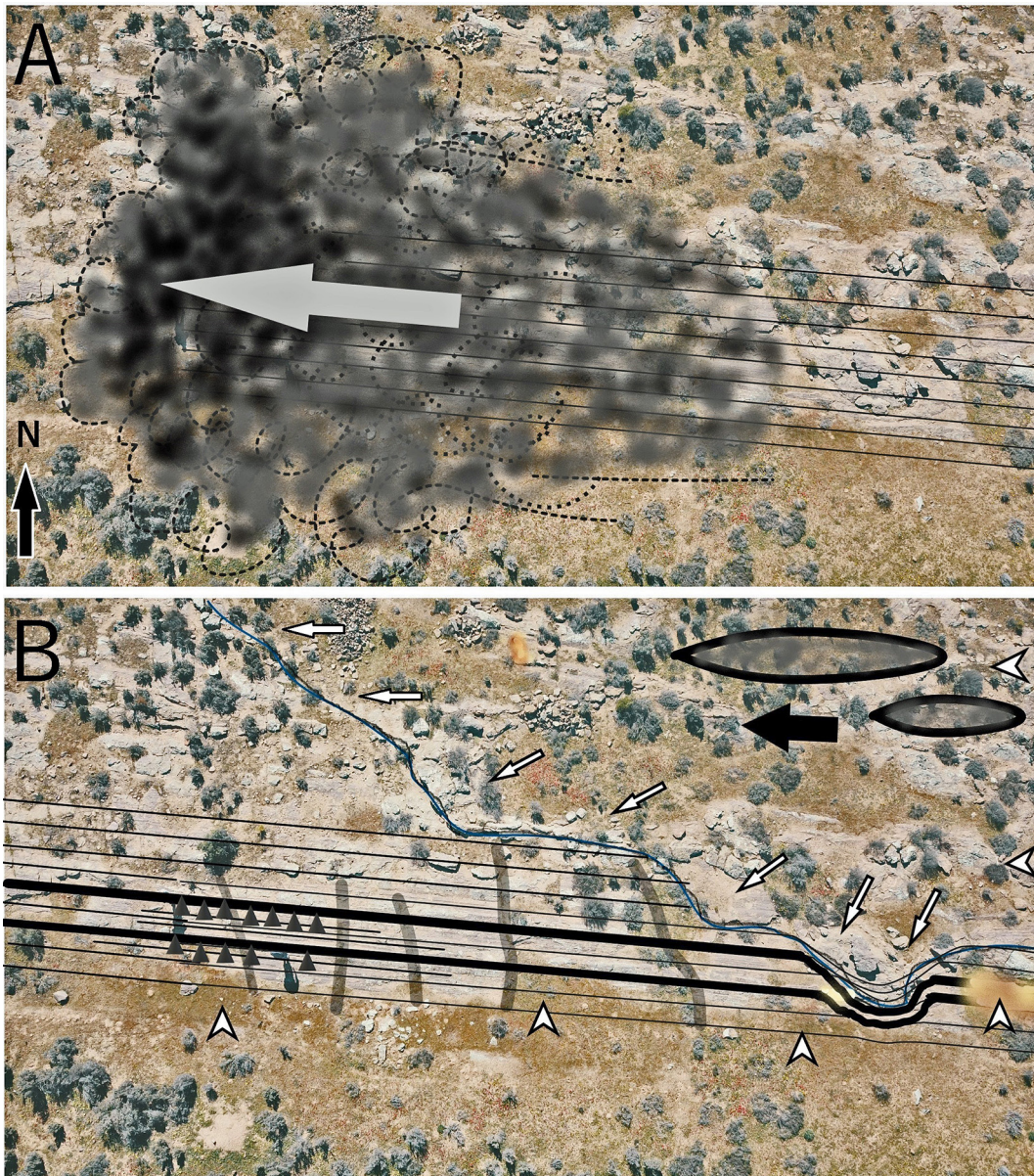

Fig. 16. Simplified drawings showing the possible sequence of events that led to the formation of the Oorlogskloof pavement area. **A –** Sediment gravity flow passed across the surface; **B –** V-shaped furrows marked as two thick parallel lines. The lower area is marked with white arrowheads. Small sandy grain flow lobes are marked as small black triangles. The direction of the sandy debris flows which pushed and deformed some of the V-shaped forms to smoother forms, marked with thin white arrows, and the outline of these sandy debris flow lobe heads is marked with a thin irregular line in front of these arrows. Linear convex 'sand bars' are depicted as two oblong structures in the upper right-hand corner (direction marked with black arrow). The 'sand bars' are outside the photograph and not exactly next to each other, but have been drawn inside the photograph. Perpendicular fractures are marked with thick, grey, almost vertical lines. Fractures are visible in Figure 13A. See text for details.

sediments, the V-shaped structures at this place were not flattened but only rounded, almost like a dough.

5. Subsequently, faulting opened up perpendicular fractures, and parts of the pavement area were downwarped by 10–30 cm. The sediments were still not lithified and in at least one place were displaced northwards over a distance of some tens of centimeters.

Whatever the exact depositional history of the Dwyka Group is, there is no unequivocal evidence of glaciation. It appears possible to exchange simply the word glaciogenic with, for instance, tectonics and sediment gravity flows. The diamictites and pavements in the area do not conform to the current paradigm of glaciation. This is especially evident by the absence of glacially formed surface microtextures (i.e., there are no F1/A1), but also by the overall appearance of the geological features of the Dwyka Group.

Dietrich et al. (2019, p. 887) noted, following the description of an area in Botswana that did not display any evidence of glaciation, that the deposits had been reinterpreted and there is an „ ... emerging view that the (Late Paleozoic Ice Age) ice mass was in fact fragmented, covering only patches of southern Gondwana". From the evidence presented here, glaciers were not only patchy, but non-existent all over South Africa, or at least did not leave any imprint on the geology in the area. The implications of these data may help resolving some paradoxes concerning Late Palaeozoic climates and inferred glaciations.

We may conclude with the words of Johan N. J. Visser, formerly of the University of the Orange Free State in South Africa and probably the foremost expert on the Dwyka Group, that: "... ancient deposits do not always correspond with Cenozoic glaciation models" (Visser, 1989a, p. 378). If the Dwyka Group was not formed by glaciation, this statement is fully understandable. The present may be the key to the past, but past interpretations are not always the solution to past geological processes.

Table 4. Geological features of Dwyka Group deposits for outcrops documented in the present study, comparing glaciogenic and mass flow features (for more details of different features, reference is made to Molén, 2017, 2021, 2022a, 2022b). Not included are structures that form by non-glaciogenic processes in a glacial environment, e.g., debris flows. Tabulated features are only those that differ much between glaciogenic and non-glaciogenic deposits. Conjectural or insignificant (not fully) documented differences from the study area are not tabulated, but discussed in the text only.

Feature	Origin		
	Glacial	Sediment gravity flow	Dwyka Group
Warm climate fossils	0–1	2	*
Streaks of different sediments/diamictites	1	2	*
Unconsolidated transported sediment	1	2	*
Pavement/striations/grooves	2	1	
parallel striations	1	2	**
soft sediment pavements	1	2	**
stacked pavements	0–1	1–2	**
regular striations	0–1	1–2	*
interlaminated sediments/traction carpet	–	1	**
Iceberg keel scour marks and mimics	2	0–1	
superposed/stacked in same direction	–	1	*
parallel striations/grooves	1	2	**
Roches moutonnés/plucking	2	(0–1)	*
uneven surfaces	0–1	1	*
Fjords, overdeepened, regular, ridged outlet	2	(0–1)	*
Dropstones/outsized clasts	2	2	
small size	1	2	*
small size compared to other sediments	–	2	*
no/little penetration	1	2	*
Surface microtextures weathered and regularly abraded	–	2	**

2nd and 3rd column: 2 = more common, 1 = less common, 0 = very rare, – = no example known, parentheses = rare or commonly displaying a distinct appearance.

The last column summarises which features are more indicative of sediment gravity flow: * = similarities to sediment gravity flow features, but not excluding a glaciogenic origin, ** = non-glaciogenic origin.

Evidence of the geological features discussed in the present paper, which are different when comparing glaciogenic and mass flow deposits, is summed up in Table 4.

Acknowledgements

References

Amblas, D., Gerber, T.P., Canals, M., Pratson, L.F., Urgeles, R., Lastras, G. & Calafat, A.M., 2011. Transient erosion in the Valencia Trough turbidite systems, NW Mediterranean Basin. *Geomorphology* 130, 173–184.

Anderson, A.M. & McLachlan, I.R., 1976. The plant record in the Dwyka and Ecca series (Permian) of the south-western half of the Great Karroo Basin, South Africa. *Palaeontologica Africana* 19, 31–42.

Baas, J.H., Tracey, N.D. & Peakall, J., 2021. Sole marks reveal deep-marine depositional process and environment: Implications for flow transformation and hybrid-event-bed models. *Journal of Sedimentary Research* 91, 986–1009.

Baiyegunhi, C. & Gwavava, O., 2016. Variations in isochore thickness of the Ecca sediments in the eastern Cape Province of South Africa, as deduced from gravity models. *Acta Geologica Sinica* 90, 1699–1712.

Bangert, B. & Von Brunn, V., 2001. Tuffaceous beds in glaciogenic argillites of the Late Palaeozoic Dwyka Group of KwaZulu-Natal, South Africa. *Journal of African Earth Sciences* 32, 133–140.

Barbolini, N., Rubidge, B. & Bamford, M.K., 2018. A new approach to biostratigraphy in the Karoo retroarc foreland system: utilising restricted-range palynomorphs and their first appearance datums for correlation. *Journal of African Earth Sciences* 140, 114–133.

Bechstädt, T., Jäger, H., Rittersbacher, A., Schweisfurth, B., Spence, G., Werner, G. & Boni, M.. 2018. The Cryogenian Ghaub Formation of Namibia – New insights into Neoproterozoic glaciations. *Earth-Science Reviews* 177, 678–714.

Bell, D., Hodgson, D.M., Pontén, A.S.M., Hansen, L.A.S., Flint, S.S. & Kane, I.A., 2020. Stratigraphic hierarchy and three-dimensional evolution of an exhumed submarine slope channel system. *Sedimentology* 67, 3259–3289.

Bennett, M.R., Doyle, P. & Mather, A.E., 1996. Dropstones: their origin and significance. *Palaeogeography, Palaeoclimatology, Palaeoecology* 121, 331–339.

Blignault, H.J. & Theron, J.N., 2015. The facies association tillite, boulder beds, boulder pavements, liquefaction structures and deformed drainage channels in the Permo-Carboniferous Dwyka Group, Elandsvlei area, South Africa. *South African Journal of Geology* 118, 157–172.

Bouma, A.H., 1964. Turbidites. [In:] A.H. Bouma & A.Brouwer (Eds): *Turbidites*. Elsevier, Amsterdam, pp. 251–256.

Brooks, H.L., Hodgson, D.M., Brunt, R.L., Peakall, J., Hofstra, M. & Flint, S.S., 2018. Deep-water channel-lobe transition zone dynamics: Processes and depositional architecture, an example from the Karoo Basin, South Africa. *Bulletin of the Geological Society of America* 130, 1723–1746.

Cape Geosites, 2014. Oorlogskloof glacial floor, Council for Geoscience, Western Cape Branch of the Geological Society of South Africa. https://c38e147f-b0d8-493b-a025-63dcdcddec22.filesusr.com/ugd/0de4b-d_0c9446dc737e43b1acfa0f0f205464ad.pdf.

Caputo, M.V. & Santos, R.O.B., 2020. Stratigraphy and ages of four Early Silurian through Late Devonian, Early and Middle Mississippian glaciation events in the Parnaíba Basin and adjacent areas, NE Brazil. *Earth-Science Reviews* 207, 103002.

Cardona, S., Wood, L.J., Dugan, B., Jobe, Z. & Strachan, L.J., 2020. Characterization of the Rapanui mass-transport deposit and the basal shear zone: Mount Messenger Formation, Taranaki Basin, New Zealand. *Sedimentology* 67, 2111–2148.

Catuneanu, O., Wopfner, H., Eriksson, P.G., Cairncross B., Rubidge, B.S., Smith, R.M.H. & Hancox, P.J., 2005. The Karoo basins of south-central Africa. *Journal of African Earth Sciences* 43, 211–253.

Cesta, J.M., 2015. *Soft-sediment slickensides in the Stockton Formation, Stockton, New Jersey.* Geological Society of America, Paper No. 45-1.

Chumakov, N.M. & Zharkov, M.A., 2002. Climate during Permian-Triassic biosphere reorganizations. Article 1: Climate of the Early Permian. *Stratigraphy and Geological Correlation* 10, 586–602.

Costa, P.J.M., Rasteiro da Silva, D., Figueirinhas, L. & Lario, J., 2019. The importance of coastal geomorphological setting as a controlling factor on microtextural signatures of the 2010 Maule (Chile) tsunami deposit. *Geologica Acta* 17, 1–10.

Craddock, J.P., Ojakangas, R.W., Malone, D.V., Konstantinou, A., Mory, A., Bauer, W., Thomas, R.J., Affinati, S.C., Pauls, K., Zimmerman, U., Botha, G., Rochas-Campos, A., dos Santos, P.R., Tohver, E., Riccomini, C., Martin, J., Redfern, J., Horstwood, M. & Gehrels, G., 2019. Detrital zircon provenance of Permo-Carboniferous glacial diamictites across Gondwana. *Earth-Science Reviews* 192, 285–316.

Crowell, J.C., 1957. Origin of pebbly mudstones. *Bulletin of the Geological Society of America* 68, 993–1010.

Cruikshank, K.M. & Aydin, A., 1995. Unweaving the joints in Entrada Sandstone, Arches National Park, Utah, U.S.A. *Journal of Structural Geology* 17, 409–421.

Dahl, T.W. & Arens, S.K.M., 2020. The impacts of land plant evolution on Earth´s climate and oxygenation state – An interdisciplinary review. *Chemical Geology* 547, 119665.

Dakin, N., Pickering, K.T., Mohrig, D. & Bayliss, N.J., 2013. Channel-like features created by erosive submarine debris flows: field evidence from the Middle Eocene Ainsa Basin, Spanish Pyrenees. *Marine and Petroleum Geology* 41, 62–71.

Deynoux, M. & Ghienne, J.-F., 2004. Late Ordovician glacial pavements revisited: a reappraisal of the origin of striated surfaces. *Terra Nova* 16, 95–101.

Deynoux, M. & Trompette, R., 1976. Discussion: Late Precambrian mixtites: glacial and/or nonglacial? Dealing especially with the mixtites of West Africa. *American Journal of Science* 276, 1302–1315.

Dietrich, P. & Hofmann, A., 2019. Ice-margin fluctuation sequences and grounding zone wedges: The record of the Late Palaeozoic ice age in the eastern Karoo Basin (Dwyka Group, South Africa). *Depositional Record* 5, 247–271.

Dietrich, P., Franchi, F., Setlhabi, L., Prevec, R. & Bamford, M., 2019. The nonglacial diamictite of Toutswemogala Hill (Lower Karoo Supergroup, Central Botswana): Implications on the extent of the Late Paleozoic ice age in the Kalahari–Karoo Basin. *Journal of Sedimentary Research* 89, 875–889.

Dietrich, P., Griffis, N.P., Le Heron, D.P., Montañez, I.P., Kettler, C., Robin, C. & Guillocheau, F., 2021. Fjord network in Namibia: A snapshot into the dynamics of the late Paleozoic glaciation. *Geology* 49. https://doi.org/10.1130/G49067.1.

Dill, R.F., 1964. Sedimentation and erosion in Scripps Submarine Canyon head. [In:] R.L. Miller (Ed.): *Papers in Marine Geology*. Macmillan, New York, pp. 23–41.

Draganits, E., Schlaf, J., Grasemann, B. & Argles, T., 2008. Giant submarine landslide grooves in the Neoproterozoic/Lower Cambrian Phe Formation, northwest Himalaya: Mechanisms of formation and palaeogeographic implications. *Sedimentary Geology* 205, 126–141.

du Toit, A.L., 1926. *The Geology of South Africa.* Oliver & Boyd, Edinburgh, pp. 205–215.

Dufresne, A.& Davies, T.R., 2009. Longitudinal ridges in mass movement deposits. *Geomorphology* 105, 171–181.

Dufresne, A., Zernack, A., Bernard, K., Thouret, J.-C. & Roverato, M., 2021. Sedimentology of volcanic debris avalanche deposits. [In:] M. Roverato, A. Dufresne & J. Procter (Eds.): *Volcanic Debris Avalanches. Advances in Volcanology*. Springer, pp. 175–210.

Dunlevey, J.N. & Smith, A.M., 2011. Sedimentological evidence for an interglacial in the Permo-Carboniferous Dwyka Group, Coedmore Quarry, Durban, South Africa. *South African Journal of Geology* 114, 159–166.

Embley, R.W., 1982. Anatomy of some Atlantic margin sediment slides and some comments on ages and mechanisms. [In:] S. Saxov & J.K. Nieuwenhuis (Eds): *Marine Slides and Other Mass Movements*. Plenum Press, New York, pp. 189–213.

Enos, P., 1969. Anatomy of flysch. *Journal of Sedimentary Research* 39, 680–723.

Evenson, E.B., Dreimanis, A. & Newsome, J.W., 1977. Subaquatic flow tills: a new interpretation for the genesis of some laminated deposits. *Boreas* 6, 115–133.

Eyles, N., 1993. Earth´s glacial record and its tectonic setting. *Earth-Science Reviews* 35, 1–248.

Eyles, N. & Januszczak, N., 2007. Syntectonic subaqueous mass flows of the Neoproterozoic Otavi Group, Namibia: where is the evidence of global glaciation? *Basin Research* 19, 179–198.

Fagereng, Å., 2014. Significant shortening by pressure solution creep in the Dwyka diamictite, Cape Fold Belt, South Africa. *Journal of African Earth Sciences* 97, 9–18.

Fedorchuk, N.D., Isbell, J.L., Griffis, N.P., Montañez, I.P., Vesely, F.F., Iannuzzi, R., Mundil, R., Yin, Q-Z., Pauls, K.N. & Rosa, E.L.M., 2019. Origin of paleovalleys on the Rio Grande do Sul Shield (Brazil): implications for the extent of late Paleozoic glaciation in west-central Gondwana. *Palaeogeography, Palaeoclimatology, Palaeoecology* 531, Part B, 108738.

Festa, A., Ogata, K., Pini, G.A., Dilek, Y. & Alonso, J.L., 2016. Origin and significance of olistostromes in the evolution of orogenic belts: a global synthesis. *Gondwana Research* 39, 180–203.

Fleisher, P.J., Lachniet, M.S., Muller, E.H. & Bailey, P.K., 2006. Subglacial deformation of trees within overridden foreland strata, Bering Glacier, Alaska. *Geomorphology* 75, 201–211.

Flint, R.F., 1961. Geological evidence of cold climate. [In:] A.E.M. Nairn (Ed.): *Descriptive Palaeoclimatology*. Interscience Publishing, New York, pp. 140–155.

Geophysical Discussion of the Royal Astronomical Society, 1960. *Geophysical journal of the Royal Astronomical Society (incorporating the Geophysical Supplement to the Monthly Notices of the R.A.S.)* 3, 127–132.

Glicken, H., 1996. *Rockslide-debris avalanche of May 18, 1980, Mount St. Helens Volcano, Washington*. U.S. Geological Survey, Open-File Report 96-677, 98 pp,

Górska, M.E., Woronko, B., Kossowski, T.M. & Pisarska-Jamroży, M., 2022. Micro-scale frost-weathering simulation – Changes in grain-size composition and influencing factors. *Catena* 212, 106106.

Götz, A.E., Ruckwied, K. & Wheeler, A., 2018. Marine flooding surfaces recorded in Permian black shales and coal deposits of the Main Karoo Basin (South Africa): implications for basin dynamics and cross-basin correlation. *International Journal of Coal Geology* 190, 178–190.

Griffis, N., Montañez, I., Mundil, R., Le Heron, D., Dietrich, P., Kettler, C., Linol, B., Mottin, T., Vesely, F., Iannuzzi, R., Huyskens, M. & Yin, Q.-Z., 2021. High-latitude ice and climate control on sediment supply across SW Gondwana during the late Carboniferous

and early Permian. *Bulletin of the Geological Society of America* 133, 2113–2124.

Haflidason, H., Sejrup, H.P., Nygård, A., Mienert, J., Bryn, P., Lien, R., Forsberg, C.F., Berg, K. & Masson, D., 2004. The Storegga Slide: architecture, geometry and slide development. *Marine Geology* 213, 201–234.

Haldorsen, S., Von Brunn, V., Maud, R. & Truter, E.D., 2001. A Weichselian deglaciation model applied to the early Permian glaciation in the northeast Karoo Basin, South Africa. *Journal of Quaternary Science* 16, 583–593.

Hancox, P.J. & Götz, A.E., 2014. South Africa's coalfields – A 2014 perspective. *International Journal of Coal Geology* 132, 170–254.

Hansen, L.A.S., Hodgson, D.M., Pontén, A., Bell, D. & Flint, S., 2019. Quantification of basin-floor fan pinchouts: examples from the Karoo Basin, South Africa. *Frontiers in Earth Science* 7, article 12.

Hawkes, L., 1943. The erratics of the Cambridge Greensand – their nature provenance and mode of transport. *Quarterly Journal of the Geological Society of London* 99, 93–104.

Horan, K., 2015. *Falkland Islands (Islas Malvinas) in the Permo-Carboniferous.* Springer Earth System Sciences, pp. 45–70.

Huber, H., Koeberl, C., Mcdonald, I. & Reimold, W.U., 2001. Geochemistry and petrology of Witwatersrand and Dwyka diamictites from South Africa: search for an extraterrestrial component. *Geochimica et Cosmochimica Acta* 65, 2007–2016.

Isbell, J.L., Cole, D.I. & Catuneanu, O., 2008. Carboniferous-Permian glaciation in the main Karoo Basin, South Africa: Stratigraphy, depositional controls, and glacial dynamics. [In:] C.R. Fielding, T.D. Frank, & J.L. Isbell (Eds): *Resolving the Late Paleozoic Ice Age in Time and Space*. Geological Society of America Special Paper 441, pp. 71–82.

Isbell, J.L., Henry, L.C., Reid, C.M & Fraiser, M.L., 2013. Sedimentology and palaeoecology of lonestone-bearing mixed clastic rocks and cold-water carbonates of the Lower Permian basal beds at Fossil Cliffs, Maria Island, Tasmania (Australia): Insight into the initial decline of the late Palaeozoic ice age. [In:] A. Gasiewicz & M. Słowakiewicz (Eds): *Palaeozoic Climate Cycles: Their Evolutionary and Sedimentological Impact*. Geological Society, London, Special Publications 376, pp. 307–341.

Isbell, J.L., Henry, L.C., Gulbranson, E., Limarino, C.O., Fraiser, M.L., Koch, Z.J., Ciccioli, P.L. & Dineen, A.A., 2012. Glacial paradoxes during the late Paleozoic ice age: evaluating the equilibrium line altitude as a control on glaciation. *Gondwana Research* 22, 1–19.

Iverson, N.R., 1991. Morphology of glacial striae: Implications for abrasion of glacier beds and fault surfaces. *Bulletin of the Geological Society of America* 103, 1308–1316.

John, B.S., 1979. The great ice age: Permo-Carboniferous. [In:] B.S. John (Ed.): *The Winters of the World*. Davies & Charles, Newton Abbot, pp. 154–172.

Johnson, M.R., Van Vuuren, C.J., Visser, J.N.J., Cole, D.I., Wickens, H.D.V., Christie, A.D.M. & Roberts, D.L.,

1997. The foreland Karoo Basin, South Africa [In:] R.C. Selley (Ed.): *African Basins, Sedimentary Basins of the World 3.* Elsevier, Amsterdam, pp. 269–317.

Kalińska, E., Lamsters, K., Karušs, J., Krievāns, M., Rečs, A. & Ješkins, J., 2022. Does glacial environment produce glacial mineral grains? Pro- and supra-glacial Icelandic sediments in microtextural study. *Quaternary International* 617, 101–111.

Kalińska-Nartiša, E., Woronko, B. & Ning, W., 2017. Microtextural inheritance on quartz sand grains from Pleistocene periglacial environments of the Mazovian Lowland, Central Poland. *Permafrost and Periglacial Processes* 28, 741–756.

Kennedy, K. & Eyles, N., 2021. Syn-rift mass flow generated 'tectonofacies' and 'tectonosequences' of the Kingston Peak Formation, Death Valley, California, and their bearing on supposed Neoproterozoic panglacial climates. *Sedimentology* 68, 352–381.

Kent, D.V. & Muttoni, G., 2020. Pangea B and the Late Paleozoic ice age. *Palaeogeography, Palaeoclimatology, Palaeoecology* 553, 109753.

Kneller, B.C., Edwards, D., McCaffrey, W.D. & Moore, R., 1991. Oblique reflection of turbidity currents. *Geology* 14, 250–252.

Kut, A.A.,Woronko, B., Spektor, V.V. & Klimova, I.V., 2021. Grain-surface microtextures in deposits affected by periglacial conditions (Abalakh High-Accumulation Plain, Central Yakutia, Russia). *Micron* 146, 103067.

Le Heron, D.P., Busfield, M.E. & Collins, A.S., 2014. Bolla Bollana boulder beds: a Neoproterozoic trough mouth fan in South Australia? *Sedimentology* 61, 978–995.

Le Heron, D.P., Heninger, M., Baal, C. & Bestmann, M., 2020. Sediment deformation and production beneath soft-bedded Palaeozoic ice sheets. *Sedimentary Geology* 408, 105761.

Le Heron, D.P, Sutcliffe, O.E., Whittington, R.J. & Craig, J., 2005. The origins of glacially related soft-sediment deformation structures in Upper Ordovician glaciogenic rocks: implication for ice-sheet dynamics. *Palaeogeography, Palaeoclimatology, Palaeoecology* 218, 75–103.

Le Heron, D.P., Dietrich, P., Busfield, M.E., Kettler, C., Bermanschläger, S. & Grasemann, B., 2019. Scratching the surface: footprint of a late Carboniferous ice sheet. *Geology* 47, 1034–1038.

Le Heron, D.P., Kettler, C., Griffis, N.P., Dietrich, P., Montañez, I.P., Osleger, D.A., Hofmann, A, Douillet, G. & Mundil, R., 2021. The Late Palaeozoic Ice Age unconformity in southern Namibia viewed as a patchwork mosaic. *Depositional Record* 00:1–17.

Lindsay, J.F., 1970. Depositional environment of Paleozoic glacial rocks in the Central Transantarctic Mountains. *Bulletin of the Geological Society of America* 81, 1149–1171.

Liu, Y. & Gastaldo, R.A., 1992. Characteristics and provenance of log-transported gravels in a Carboniferous channel deposit. *Journal of Sedimentary Petrology* 62, 1072–1083.

Loope, D.B. & Burberry, C.M., 2018. Sheeting joints and polygonal patterns in the Navajo Sandstone, southern

Utah: Controlled by rock fabric, tectonic joints, buckling, and gullying. *Geosphere* 14, 1818–1836.

Mahaney, W.C., 2002. *Atlas of Sand Grain Surface Textures and Applications*. Oxford University Press, New York, 237 pp.

Major, J.J., Pierson, T.C. & Scott, K.M., 2005. Debris flows at Mount St. Helens, Washington, USA. [In:] M. Jakob, & O. Hungr (Eds): *Debris-Flow Hazards and Related Phenomena*. Praxis/Springer, Berlin, pp. 685–731.

Mangerud, J., Hughes, A.L.C., Sæle, T.H. & Svendsen, J.I., 2019. Ice-flow patterns and precise timing of ice sheet retreat across a dissected fjord landscape in western Norway. *Quaternary Science Reviews* 214, 139–163.

Martin, H., 1981. The late Palaeozoic Gondwana glaciation. *Geologische Rundschau* 70, 480–496.

Master, S., 2012. Hertzian fractures in the sub-Dwyka Nooitgedacht striated pavement, and implications for the former thickness of Karoo strata near Kimberley, South Africa. *South African Journal of Geology* 115, 561–576.

McLoughlin, S., 2011. Glossopteris – insights into the architecture and relationships of an iconic Permian Gondwanan plant. *Journal of the Botanical Society of Bengal* 65, 1–14.

Mitchell, N.C., 2006. Morphologies of knickpoints in submarine canyons. *Bulletin of the Geological Society of America* 18, 589–605.

Molén, M.O., 2014. A simple method to classify diamicts by scanning electron microscope from surface microtextures. *Sedimentology* 61, 2020–2041.

Molén, M.O., 2017. The origin of Upper Precambrian diamictites; Northern Norway: A case study applicable to diamictites in general, *Geologos* 23, 163–181.

Molén, M.O., 2021. Field evidence suggests that the Palaeoproterozoic Gowganda Formation in Canada is non-glacial in origin. *Geologos* 27, 73–91.

Molén, M.O., 2022a. Glaciation or not? An analytic review of features of glaciation and sediment gravity flows: introducing a methodology for field research. Submitted. https://www.essoar.org/doi/10.1002/essoar.10510880.1

Molén, M.O., 2022b. Glaciation and mass flows: patterns, processes and models – a short analytic review. In progress.

Montañez, I.P. & Poulsen, C.J., 2013. The Late Paleozoic Ice Age: An evolving paradigm. *Annual Review of Earth and Planetary Sciences* 41, 629–656.

Montañez, I.P., McElwain, J.C., Poulsen, C.J., White, J.D., DiMichele, W.A., Wilson, J.P., Griggs, G. & Hren, M.T., 2016. Climate, pCO_2 and terrestrial carbon cycle linkages during late Palaeozoic glacial-interglacial cycles. *Nature Geoscience* 9, 824–828.

Myers, T.S., 2016. CO_2 and late Palaeozoic glaciation. *Nature Geoscience* 9, 803–804.

Norman, N., 2013. *Geology of the Beaten Track*. Struik Nature, Cape Town, 256 pp.

Normandeau, A., Lajeunesse, P. & St-Onge, G., 2015. Submarine canyons and channels in the Lower St. Lawrence Estuary (Eastern Canada): Morphology, classification and recent sediment dynamics. *Geomorphology* 241, 1–18.

Ortiz-Karpf, A., Hodgson, D.M., Jackson, C.A.-L. & McCaffrey, W.D., 2017. Influence of seabed morphology and substrate composition on mass-transport flow processes and pathways: insights from the Magdalena Fan, offshore Colombia. *Journal of Sedimentary Research* 87, 189–209.

Passchier, S., Hansen, M.A. & Rosenberg, J., 2021. Quartz grain microtextures illuminate Pliocene periglacial sand fluxes on the Antarctic continental margin. *Depositional Record* 7, 564–581.

Peakall, J., Best, J., Baas, J.H., Hodgson, D.M., Clare, M.A., Talling, P.T., Dorrell, R.M. & Lee, D.R., 2020. An integrated process-based model of flutes and tool marks in deep-water environments: Implications for palaeohydraulics, the Bouma sequence and hybrid event beds. *Sedimentology* 67, 1601–1666.

Petit, J.P. & Laville, E., 1987. Morphology and microstructures of hydroplastic slickensides in sandstone. [In:] M.E. Jones & R.M. Preston (Eds): *Deformation of Sediments and Sedimentary Rocks*. Geological Society, London, Special Publications 29, pp. 107–121.

Pickering, K.T, Underwood, M.B. & Taira, A., 1992. Open-ocean to trench turbidity-current flow in the Nankai Trough: flow collapse and reflection. *Geology* 20, 1099–1102.

Piper, D.J.W., Cochonat, P. & Morrison, M.L., 1999. The sequence of events around the epicentre of the 1929 Grand Banks earthquake: initiation of debris flows and turbidity current inferred from sidescan sonar. *Sedimentology* 46, 79–97.

Potter, P.E. & Pettijohn, F.J., 1963. *Paleocurrents and basin analysis*. Springer, Berlin, 296 pp.

Price, P.H., 1932. Erratic boulders in Sewell Coal of West Virginia. *Journal of Geology* 40, 62–73.

Puga Bernabéu, Á., Webster, J.M., Beaman, R.J., Thran, A., López Cabrera, J., Hinestrosa, G. & Daniell, J., 2020. Submarine landslides along the mixed siliciclastic carbonate margin of the great barrier reef (offshore Australia). [In:] K. Ogata, A. Festa, & G.A. Pini (Eds): *Submarine Landslides: Subaqueous Mass Transport Deposits from Outcrops to Seismic Profiles*. Geophysical Monograph 246, Wiley & Sons, pp. 313–337.

Rampino, M.R., 2017. Are some tillites impact-related debris-flow deposits? *Journal of Geology* 125, 155–164.

Ruban, D.A., Al-Husseini, M.I. & Iwasaki, Y., 2007. Review of Middle East Paleozoic plate tectonics. *GeoArabia* 12, 35–56.

Ryder, J. M. & Thomson, B., 2011. Neoglaciation in the southern Coast Mountains of British Columbia: Chronology prior to the late Neoglacial maximum. *Canadian Journal of Earth Science* 23, 273–287.

Sandberg, C.G.S., 1928. The origin of the Dwyka Conglomerate of South Africa and other "glacial" deposits. *Geological Magazine* 65, 117–138.

Savage, N.M., 1972. Soft-dediment glacial grooving of Dwyka Age in South Africa. *Journal of Sedimentary Petrology* 42, 307–308.

Scheffler, K., Hoernes, S. & Schwark, L., 2003. Global changes during Carboniferous–Permian glaciation of Gondwana: Linking polar and equatorial climate evolution by geochemical proxies. *Geology* 31, 605–608.

Scheiber-Enslin, S.E., Ebbing, J. & Webb, S.J., 2015. New depth maps of the main Karoo Basin, used to explore the Cape isostatic anomaly, South Africa. *South African Journal of Geology* 118, 225–248.

Schermerhorn, L.J.G., 1970. Saharan ice. *Geotimes* 15, 7–8.

Schermerhorn, L.J.G., 1971. Upper Ordovician glaciation in Northwest Africa? Discussion. *Bulletin of the Geological Society of America* 82, 265–268.

Schermerhorn, L.J.G., 1974. Late Precambrian mixtites: glacial and/or nonglacial? *American Journal of Science* 274, 673–824.

Schermerhorn, L.J.G., 1976a. Reply. *American Journal of Science* 276, 375–384.

Schermerhorn, L.J.G., 1976b. Reply. *American Journal of Science* 276, 1315–1324.

Schermerhorn, L.J.G., 1977. Late Precambrian glacial climate and the Earth´s obliquity – a discussion. *Geological Magazine* 114, 57–64.

Schneider, J.L. & Fisher, R.V., 1998. Transport and emplacement mechanisms of large volcanic debris avalanches: evidence from the northwest sector of Cantal Volcano (France). *Journal of Volcanology and Geothermal Research* 83, 141–165.

Scotese, C.R., Song, H., Mills, B.J.W. & van der Meer, D.G., 2021. Phanerozoic paleotemperatures: The earth´s changing climate during the last 540 million years. *Earth-Science Reviews* 215, 103503.

Scott, K.M., 1988. *Origin, Behavior and Sedimentology of Lahars and Lahar-runout Flows in the Toutle-cowlitz River System.* U.S. Geological Survey Professional Paper 1447A, 76 pp.

Shanmugam, G., 2016. Submarine fans: a critical retrospective (1950–2015). *Journal of Palaeogeography* 5, 110–184.

Shanmugam, G., 2019. Reply to discussions by Zavala (2019) and by Van Loon, Hüeneke, and Mulder (2019) on Shanmugam, G. (2018), Journal of Palaeogeography, 7 (3): 197–238): 'the hyperpycnite problem'. *Journal of Palaeogeography* 8, 31.

Shanmugam, G., 2021. *Mass Transport, Gravity Flows, and Bottom Currents.* Elsevier, 571 pp.

Shanmugam, G., Lehtonen, L.R., Straume, T., Syvertsen, S.E., Hodgkinson, R.J. & Skibej, M., 1994. Slump and debris-flow dominated upper slope facies in the Cretaceous of the Norwegian and Northern North Seas (61–67°N): implications for sand distribution. *AAPG Bulletin* 78, 910–937.

Shepard, F.P. & Dill, R.F., 1966. *Submarine Canyons and Other Sea Valleys.* Rand McNally, Chicago, 381 pp.

Simms, M.J., 2007. Uniquely extensive soft-sediment deformation in the Rhaetian of the UK: evidence for earthquake or impact? *Palaeogeography, Palaeoclimatology, Palaeoecology* 244, 407–423.

Slater, G., du Toit, A.L. & Haughton, S.H., 1932. The glaciated surfaces of Nooitgedacht, near Kimberley, and the Upper Dwyka boulder shales of the eastern part of Griqualand West (Cape Province), 1929. *Transactions of the Royal Society of South Africa* 20, 301–325.

Somelar, P., Vahur, S., Hamilton, T.S., Mahaney, W.C., Barendregt, R.W. & Costa, P. 2018. Sand coatings in paleosols: evidence of weathering across the Plio-Pleistocene boundary to modern times on Mt. Kenya. *Geomorphology* 317, 91–106.

Stavrakis, N., 1986. Sedimentary environments and facies of the Orange Free State coalfield. [In:] C.R. Anhaeusser & S. Maske (Eds): *Mineral Deposits of Southern Africa vols. I and II.* Geological Society of South Africa, Johannesburg, pp. 1939–1952.

Stavrakis, N. & Smyth, M., 1991. Clastic sedimentary environments and organic petrology of coals in the Orange Free State, South Africa. *International Journal of Coal Geology* 18, 1–16.

Stratten, T. & Humphreys, A.J.B., 1974. Extensive glacial pavement of Dwyka age near Douglas, Cape Province. *South African Journal of Science* 70, 44–45.

Talling, P.J., Masson, D.G., Sumner, E.J. & Malgesini, G., 2012. Subaqueous sediment density flows: depositional processes and deposit types. *Sedimentology* 59, 1937–2003.

Talling, P.J., Wynn, R.B., Masson, D.G., Frenz, M., Cronin, B.T., Schiebel, R, Akhmetzhanov, A.M., Dallmeier-Tiessen, S., Benetti, S., Weaver, P.P.E., Georgiopoulou, A., Zühlsdorff, C. & Amy, L.A., 2007. Onset of submarine debris flow deposition far from original giant landslide. *Nature* 450, 541–544.

Talling, P.J., Allin, J., Armitage, D.A., Arnott, R.W.C., Cartigny, M.J.B., Clare, M.A., Felletti, F., Covault, J.A., Girardclos, S., Hansen, E., Hill, P.H., Hiscott, R.N., Hogg, A.J., Clarke, J.H., Jobe, Z.R., Malgesini, G., Mozzato, A., Naruse, H., Parkinson, S., Peel, F.J., Piper, D.J., Pope, E., Postma, G., Rowley, P., Sguazzini, A., Stevenson, C.J., Sumner, E.J., Sylvester, Z., Watts, C. & Xu, J., 2015. Key future directions for research on turbidity currents and their deposits. *Journal of Sedimentary Research* 85, 153–169.

Tavener-Smith, T. & Mason, T.R., 1983. A late Dwyka (Early Permian) varvite sequence near Isandlwana, Zululand, South Africa. *Palaeogeography, Palaeoclimatology, Palaeoecology* 41, 233–249.

Van der Westhuizen, W.A., de Bruiyn, H. & Meintjes, P.G., 2006. The Ventersdorp Supergroup. [In:] M.R. Johnson, C.R. Anhaeusser & R.J. Thomas (Eds): *The Geology of South Africa.* Geological Society of South Africa, Johannesburg, pp. 187–208.

Vesely, F.F., Rodrigues, M.C.N.L., da Rosa, E.L.M., Amato, J.A., Trzaskos, B., Isbell, J.L. & Fedorchuk, N.D., 2018. Recurrent emplacement of non-glacial diamictite during the late Paleozoic ice age. *Geology* 46, 615–618.

Visser, J.N.J., 1981. Carboniferous topography and glaciation in the North-Western part of the Karoo Basin, South Africa. *Annals of the Geological Survey of South Africa* 15, 13–24.

Visser, J.N.J., 1982. Upper Carboniferous glacial sedimentation in the Karoo Basin near Prieska, South Africa. *Palaeogeography, Palaeoclimatology, Palaeoecology* 38, 63–92.

Visser, J.N.J., 1983a. Glacial marine sedimentation in the Late Paleozoic Karoo Basin, Southern Africa. [In:] B.F. Molnia (Ed.): *Glacial-Marine Sedimentation.* Plenum Press, New York, pp. 667–701.

Visser, J.N.J., 1983b. The problems of recognizing ancient subaqueous debris flow deposits in glacial sequences. *Transactions of the Geological Society of South Africa* 86, 127–135.

Visser, J.N.J., 1986. Lateral lithofacies relationships in the glacigene Dwyka Formation in the western and central parts of the Karoo Basin. *Transactions of the Geological Society of South Africa* 89, 373–383.

Visser, J.N.J., 1987. The palaeogeography of part of southwestern Gondwana during the Permo-Carboniferous glaciation. *Palaeogeography, Palaeoclimatology, Palaeoecology* 61, 205–219.

Visser, J.N.J., 1988. A Permo-Carboniferous tunnel valley system east of Barklay West, Northern Cape Province. *South African Journal of Geology* 91, 350–357.

Visser, J.N.J., 1989a. The Permo-Carboniferous Dwyka Formation of Southern Africa: deposition by a predominantly subpolar marine ice sheet. *Palaeogeography, Palaeoclimatology, Palaeoecology* 70, 377–391.

Visser, J.N.J., 1989b. Stone orientation in basal glaciogenic diamictite: four examples from the Permo-Carboniferous Dwyka Formation, South Africa. *Journal of Sedimentary Petrology* 59, 935–943.

Visser, J.N.J., 1990. Glacial bedforms at the base of the Permo-Carboniferous Dwyka Formation along the western margin of the Karoo Basin, South Africa. *Sedimentology* 37, 231–245.

Visser, J.N.J., 1994. The interpretation of massive rain-out and debris-flow diamictites from the glacial marine environment. [In:] M. Deynoux, J.M.G. Miller, E.W. Domack, N. Eyles, I.J. Fairchild & G.M. Young (Eds): *Earth´s Glacial Record.* Cambridge University Press, Cambridge, pp. 83–94.

Visser, J.N.J., 1996. A Late Carboniferous subaqueous glacial valley fill complex: Fluctuations in meltwater output and sediment flux. *South African Journal of Geology* 99, 285–291.

Visser, J.N.J., 1997. Deglaciation sequences in the Permo-Carboniferous Karoo and Kalahari basins of southern Africa: a tool in the analysis of cyclic glaciomarine basin fills. *Sedimentology* 44, 507–521.

Visser, J.N.J. & Kingsley, C.S., 1982. Upper Carboniferous glacial valley sedimentation in the Karoo Basin, Orange Free State. *Transactions of the Geological Society of South Africa* 85, 71–79.

Visser, J.N.J. & Loock, J.C. 1982. An investigation of the basal Dwyka tillite in the southern part of the Karoo Basin, South Africa. *Transactions of the Geological Society of South Africa* 85, 179–187.

Visser, J.N.J. & Loock, J.C., 1988. Sedimentary facies of the Dwyka Formation associated with the Nooitgedacht Glacial Pavements, Barkly West District. *South African Journal of Geology*, 91, 38–48.

Visser, J.N.J., Colliston, W.P. & Terreblanche, J.C., 1997b. The origin of soft-sediment deformation structures in Permo-Carboniferous glacial and proglacial beds, South Africa. *Journal of Sedimentary Petrology* 54, 1183–1196.

Visser, J.N.J., Loock, J.C. & Colliston, W.P., 1987. Subaqueous outwash fan and esker sandstones in the Permo-Carboniferous Dwyka Formation of South Africa. *Journal of Sedimentary Petrology* 57, 467–478.

Visser, J.N.J., van Niekerk, B.N. & van der Merwe, S.W., 1997a. Sediment transport of the late Palaeozoic glacial Dwyka Group in the southwestern Karoo Basin. *South African Journal of Geology* 100, 223–236.

Von Brunn, V., 1994. Glaciogenic deposits of the Permo-Carboniferous Dwyka Group in the eastern region of the Karoo Basin, South Africa. [In:] M. Deynoux, J.M.G. Miller, E.W. Domack, N. Eyles, I.J. Fairchild & G.M. Young (Eds.): *Earth´s Glacial Record*. Cambridge University Press, Cambridge, pp. 60–69.

Von Brunn, V. 1996. The Dwyka Group in the northern part of Kwazulu/Natal, South Africa: sedimentation during late Palaeozoic deglaciation. *Palaeogeography, Palaeoclimatology, Palaeoecology* 125, 141–163.

Vrolijk, P.J., Urai, J.L. & Kettermann, M., 2016. Clay smear: Review of mechanisms and applications. *Journal of Structural Geology* 86, 95–152.

Whipple, K.X., Hancock, G.S. & Anderson, R.S., 2000. River incision into bedrock: Mechanics and relative efficacy of plucking, abrasion and cavitation. *Bulletin of the Geological Society of America* 112, 490–503.

Wilkins, S.J., Gross, M.R., Wacker, M., Eyal, Y. & Engelder, T., 2001. Faulted joints: kinematics, displacement – length scaling relations and criteria for their identification. *Journal of Structural Geology* 23, 315–327.

Woronko, B., 2016. Frost weathering versus glacial grinding in the micromorphology of quartz sand grains: Processes and geological implications. *Sedimentary Geology* 335, 103–119.

Yincan., Y. et al., 2017. *Marine Geo-Hazards in China*. China Ocean Press, Elsevier, pp. 193–194.

Zavala, C., 2019. The new knowledge is written on sedimentary rocks – a comment on Shanmugam's paper "The hyperpycnite problem". *Journal of Palaeogeography* 8, 23.

Zavala, C., 2020. Hyperpycnal (over density) flows and deposits. *Journal of Palaeogeography* 9, 17.

Zavala, C. & Arcuri, M., 2016. Intrabasinal and extrabasinal turbidites: origin and distinctive characteristics. *Sedimentary Geology* 337, 36–54.